AD_____

Award Number: DAMD17-99-1-9548

TITLE: NF2 in Hrs-Mediated Signal Transduction

PRINCIPAL INVESTIGATOR: Stefan M. Pulst, M.D.

CONTRACTING ORGANIZATION: Cedars-Sinai Medical Center
Los Angeles, California 90048

REPORT DATE: November 2002

TYPE OF REPORT: Annual

PREPARED FOR: U.S. Army Medical Research and Materiel Command
Fort Detrick, Maryland 21702-5012

REPORT DOCUMENTATION PAGE

Form Approved
OMB No. 074-0188

1. AGENCY USE ONLY (Leave blank)	2. REPORT DATE	3. REPORT TYPE AND DATES COVERED
	November 2002	Annual (1 Oct 01 - 1 Oct 02)

4. TITLE AND SUBTITLE
NF2 in Hrs-Mediated Signal Transduction

5. FUNDING NUMBERS
DAMD17-99-1-9548

6. AUTHOR(S) :
Stefan M. Pulst, M.D.

7. PERFORMING ORGANIZATION NAME(S) AND ADDRESS(ES)
Cedars-Sinai Medical Center
Los Angeles, California 90048

E-Mail: Pulst@CSHS.org

8. PERFORMING ORGANIZATION REPORT NUMBER

9. SPONSORING / MONITORING AGENCY NAME(S) AND ADDRESS(ES)
U.S. Army Medical Research and Materiel Command
Fort Detrick, Maryland 21702-5012

10. SPONSORING / MONITORING AGENCY REPORT NUMBER

11. SUPPLEMENTARY NOTES
Original contains color plates: All DTIC reproductions will be in black and white.

12a. DISTRIBUTION / AVAILABILITY STATEMENT
Approved for Public Release; Distribution Unlimited

12b. DISTRIBUTION CODE

13. ABSTRACT ***(Maximum 200 Words)*** We have identified Hrs (hepatocyte growth factor-regulated tyrosine kinase substrate) as an NF2 binding protein using the yeast two-hybrid system. Hrs is also known to interact with STAM (signal transduction adaptor molecule. Hrs appears to have growth suppressing functions at least in part mediated via binding to STAM with a resulting reduction in DNA synthesis. Progress is discussed in order of the three specific aims that were proposed originally:

1) Regulated overexpression of HRS in rat schwannoma cells results in similar effects as overexpression of schwannomin. This includes growth inhibition, decreased motility and abnormalities in cell spreading (Gutmann et al. 2001).
2) A recently emerging function for Hrs is the sorting of endosomes containing EGR-receptor. We have begun to examine this effect in RT4 cells overexpressing Hrs or schwannomin.
3) We have begun to generate mouse embryonic fibroblast cell lines that express schwannomin or HRS under the control of the tet-regulatable promotor. These lines will be used to examine the effects of overexpression of either protein on proliferation and STAT signaling.

14. SUBJECT TERMS
merlin, schwannomin, yeast two-hybrid system, signal transduction, tumor suppressor proteins, Hrs

15. NUMBER OF PAGES
38

16. PRICE CODE

17. SECURITY CLASSIFICATION OF REPORT	18. SECURITY CLASSIFICATION OF THIS PAGE	19. SECURITY CLASSIFICATION OF ABSTRACT	20. LIMITATION OF ABSTRACT
Unclassified	Unclassified	Unclassified	Unlimited

Table of Contents

Title	NF2 in Hrs-mediated signal transduction
PI Name	Stefan-M. Pulst
Key Words	Merlin, Schwannomin, Yeast two-hybrid system, Signal transduction, Tumor suppresser proteins, Hrs

Introduction

Germline mutations in the neurofibromatosis type 2 (NF2) gene predispose to tumors of multiple types. We have identified Hrs (hepatocyte growth factor-regulated tyrosine kinase substrate) as an NF2 binding protein using the yeast two-hybrid system. In previous years we have used the yeast two-hybrid and in vitro binding assays to fine-map the binding domains in Hrs and schwannomin. This was followed by examining the functional interactions of the two proteins. The ultimate goal of this research is to dissect schwannomin-Hrs-STAM interaction and to understand the role of schwannomin in STAM-mediated signaling in Jak/STAT pathways. This will pave the way for the identification of novel drug targets for the treatment of patients with NF2 and for patients with surgically inaccessible meningiomas and ependymomas.

Body

Specific Aim 1: Further characterization of binding domains in Hrs, schwannomin, and STAM

Task 1: Months 1-12 Fine-mapping of interacting domains in Hrs and schwannomin. **Completed**

Task 2: Months 6-18 Analysis of STAM - schwannomin interaction. **Completed**

Task 3: Months Three hybrid assays for Hrs-STAM-schwannomin interaction.

Task 4: Months 18-24 Interaction analysis of Hrs isoforms. **Completed**

Task 5: Months 28-24 Interaction analysis of rat isoform Hrs-2. **Abandoned, because it is now known that the previously reported cDNA by the Scheller group contained a sequence error. This isoform is identical to our isoform 1.**

Task 6: Months 24-30 Isolation of human Hrs-2 isoforms **Completed**

Specific Aim 2: Distribution of Hrs, STAM and schwannomin in normal cells and NF2 tumors

Task 1: Months 6-12 Cellular distribution of schwannomin and Hrs in normal Schwann cells, schwannomas, meningiomas, and ependymomas. **Completed**

Task 2: Months 12-18 Determination of colocalization of schwannomin, Hrs, and STAM in cell lines. **Completed**

Task 3: Months 18-30 Overexpression of Hrs and/or schwannomin as GFP/BFP fusion proteins.

We have completed these studies in RT4 and STS cells, but will now use NF2- and Hrs-deficient cell lines to continue these studies.

Specific Aim 3: Schwannomin in Hrs-mediated signaling

Task 1: Months 1-12 Study of Hrs proliferative effects of Hrs in STS26T cells. **Completed**

Task 2: Months 12-24 Schwannomin and Hrs overexpression in mouse NF2 deficient cell lines.

We are planning to finish these experiments in the last year of funding. We now have in hand human NF2- deficient schwannoma cells, *Hrs*-deficient mouse embryonic fibroblasts, and *Nf2*-deficient mouse

embryonic fibroblasts. These resources will permit the execution of unique experiments that will define the roles of Hrs and NF2 expressed as single molecules or in combination.

Task 3: Months 12-24 Proliferative effects of schwannomin and Hrs fragments bearing deletions of their respective binding sites including STAM binding sites. **Completed**

Task 4: Months 18-36 Analysis of Jak/STAT pathways after schwannomin and Hrs transfection. **Completed**

Task 5: Months 24-36 Analysis of BAF-B03 cells after NF2 transfection including NF2 constructs bearing deletions or missense mutations.

We will employ the established model by Asao et al (1997) used to analyze Hrs and STAM function after treatment of BAF-B03 cells with HGF, and GM-CSF. We will monitor proliferative responses after introduction of wildtype schwannomin instead of wildtype Hrs as they had done.

Key Research Accomplishments

- In this funding cycle we determined the effects of Nf2 missense mutations on schwannomin interactions (Scoles et al., 2002a appended).
- We also analyzed how the NF2 tumor suppressor schwannomin and its interacting protein HRS regulate STAT signaling (Scoles et al., 2002b, appended).
- Finally, in collaboration with Dr. D. Gutmann, we determined that NF2 likely acts upstream of Hrs (Sun et al., 2002, appended).
- We have generated novel cell lines that express NF2 and Hrs in an inducible fashion.

Reportable outcomes

Abstracts published:

Scoles, D.R., Chen, M.S., and Pulst, S.M. Effects of NF2 missense mutations on schwannomin interactions. *Biochemical Biophysical Research Communications* 290(1):366-374; 2002.

Sun, C.X., Haipek, C., Scoles, D.R., Pulst, S.M., Giovannini, M., Komada, M., and Gutmann, D.H. Functional analysis of the relationship between the neurofibromatosis 2 (NF2) tumor suppressor and its binding partner, hepatocyte growth factor-regulated tyrosine kinase substrate (HRS/HGS). *Human Molecular Genetics* 11(25), Dec 1, 2002 (In Press).

Scoles, D.R., Nguyen, V.D., Qin, Y., Sun, C.X., Morrison, H., Gutmann, D.H., and Pulst, S.M. Neurofibromatosis 2 (NF2) tumor suppressor schwannomin and its interacting protein HRS regulate STAT signaling. *Human Molecular Genetics* 11(25), Dec 1, 2002 (In Press).

Scoles, D.R., Nguyen, V.D., Qin, Y., Sun, C.X., Morrison, H., Gutmann, D.H., and Pulst, S.M. Neurofibromatosis 2 (NF2) tumor suppressor schwannomin and its interacting protein HRS regulate STAT signaling. *Human Molecular Genetics* 11(25), Dec 1, 2002 (In Press).

Abstract presentations:

Scoles, D.R., Nguyen, V., Lam, S., and Pulst, S.M. The NF2 tumor suppressor schwannomin interacts with p110, a coponent of the eukaryotic initiation factor 3 (eIF3). *Neurology* (Suppl. 3) 58:A11 (2002).(Annual AAN meeting 2002)

The NF2 tumor suppressor schwannomin interacts with the eukaryotic initiation factor 3 (eIF3) subunit p110Daniel R Scoles, Vu D. Nguyen, Samuel Lam, Yun Qin, Stefan M. Pulst
Burns and Allen Research Institute and Division of Neurology, Cedars-Sinai Medical Center, and UCLA School of Medicine, Los Angeles, California (ASCB 42nd Annual Meeting, December 14-18, 2002, San Francisco.)

Publications:

Scoles DR, Nguyen VD, Qin Y, Sun CX, Morrison H, Gutmann DH, Pulst SM.
Neurofibromatosis 2 (NF2) tumor suppressor schwannomin and its interacting protein HRS regulate STAT signaling.Hum Mol Genet. 2002 Dec 1;11(25):3179-3189.
Sun CX, Haipek C, Scoles DR, Pulst SM, Giovannini M, Komada M, Gutmann DH.
Functional analysis of the relationship between the neurofibromatosis 2 tumor suppressor and its binding partner, hepatocyte growth factor-regulated tyrosine kinase substrate.Hum Mol Genet. 2002 Dec 1;11(25):3167-3178.

Scoles, D.R., Chen, M.S., and Pulst, S.M. Effects of NF2 missense mutations on schwannomin interactions. *Biochemical Biophysical Research Communications* 290(1):366-374; 2002.

Human Molecular Genetics, 2002, Vol. 11, No. 25 1–12

Functional analysis of the relationship between the neurofibromatosis 2 tumor suppressor and its binding partner, hepatocyte growth factor-regulated tyrosine kinase substrate

Chun-Xiao Sun[1], Carrie Haipek[1], Daniel R. Scoles[2], Stefan M. Pulst[2], Marco Giovannini[3], Masayuki Komada[4] and David H. Gutmann[1,*]

[1]Department of Neurology, Washington University School of Medicine, St Louis, MO 63110, USA, [2]Neurogenetics Laboratory, CSMC Burns and Allen Research Institute, Cedars-Sinai Medical Center, Los Angeles, CA 90048, USA, [3]INSERM U434, Fondation Jean Dausset CEPH, 75010 Paris, France and [4]Department of Biological Sciences, Tokyo Institute of Technology, Yokohama, Japan

Received July 30, 2002; Revised and Accepted October 2, 2002

Individuals with neurofibromatosis 2 (NF2) inherited tumor predisposition syndrome are prone to the development of nervous system tumors, including schwannomas and meningiomas. The *NF2* tumor suppressor protein, merlin or schwannomin, inhibits cell growth and motility as well as affecting actin cytoskeleton-mediated processes. Merlin interacts with several proteins that might mediate merlin growth suppression, including hepatocyte growth factor-regulated tyrosine kinase substrate (HRS or HGS). Previously, we demonstrated that regulated overexpression of HRS in RT4 rat schwannoma cells had the same functional consequences as regulated overexpression of merlin. To determine the functional significance of this interaction, we generated a series of HRS truncated mutants and defined the regions of HRS required for merlin binding and HRS growth suppression. The HRS domain required for merlin binding was narrowed to a region (residues 470–497) containing the predicted coiled-coil domain whereas the major domain responsible for HRS growth suppression was distinct (residues 498–550). To determine whether merlin growth suppression required HRS, we demonstrated that merlin inhibited growth in *HRS*$^{+/+}$, but not *HRS*$^{-/-}$ mouse embryonic fibroblast cells. In contrast, HRS could suppress cell growth in the absence of *Nf2* expression. These results suggest that merlin growth suppression requires HRS expression and that the binding of merlin to HRS may facilitate its ability to function as a tumor suppressor.

INTRODUCTION

Neurofibromatosis 2 (NF2) is an autosomal dominant inherited tumor predisposition syndrome in which affected individuals are prone to the development of specific nervous system tumors (1). The hallmark central nervous system tumor in NF2 is the schwannoma, typically involving both eighth cranial nerves (bilateral vestibular schwannomas). Continued growth of these tumors leads to deafness and balance problems. In addition to bilateral vestibular schwannomas, schwannomas can occur on other cranial or peripheral nerves throughout the body. The second most common tumor in NF2 is the meningioma, arising from leptomeningeal cap cells and is seen in 50% of affected individuals. Lastly, ependymomas and, less commonly, astrocytomas are also observed in NF2 patients.

The *NF2* gene was identified by positional cloning in 1993 and found to encode a 595 amino acid protein termed merlin or schwannomin (2,3). Merlin contains three predicted structurally important regions, including an amino terminal FERM domain (residues 1–302), a central alpha helical region (residues 303–479) and a unique carboxyl terminus (residues 480–595). Based on this structure, merlin has been classified as a member of the Protein 4.1 subfamily of proteins that includes ezrin, radixin and moesin (ERM proteins) (4). These proteins are proposed to link the actin cytoskeleton to cell surface glycoproteins. While ERM proteins have not been directly implicated in growth regulation, ezrin has been shown to modulate apoptosis in particular cell types (5). Like other ERM proteins, merlin binds to actin and is associated with the actin cytoskeleton (6). However, merlin has a different subcellular

*To whom correspondence should be addressed at: Department of Neurology, Washington University School of Medicine, Box 8111, 660 South Euclid Avenue, St Louis, MO 63110, USA. Tel: +1 3143627379; Fax: +1 3143622388; Email: gutmannd@neuro.wustl.edu

distribution than other ERM proteins in peripheral nerve Schwann cells, reinforcing the idea that merlin is a unique member of this Protein 4.1 family of proteins (7,8).

Since individuals with NF2 are at increased risk of developing specific nervous system tumors, the *NF2* gene has been hypothesized to function as a tumor suppressor (9). Support for this classification derives from studies demonstrating germline mutations in the *NF2* gene in NF2 patients and bi-allelic inactivation of *NF2* in NF2-associated tumors, including schwannomas, ependymomas and meningiomas (10–12). Moreover, re-expression of the *NF2* gene in merlin-deficient meningioma cells *in vitro* and schwannoma cells both *in vitro* and *in vivo* results in growth suppression (13,14). In contrast, regulated expression of merlin containing missense NF2 patient mutations has no effect on cell growth either *in vitro* or *in vivo* (15). Merlin loss is also observed in nearly all sporadic schwannomas and over half of sporadic meningiomas, suggesting that the *NF2* tumor suppressor plays a more general role in the molecular pathogenesis of these tumors (16–19).

Clues to the mechanism of action of merlin have derived from several different studies. Mice with a targeted mutation in the *Nf2* gene develop malignant tumors that exhibit a highly metastatic phenotype (20). This finding suggested that merlin might normally regulate both cell proliferation and actin cytoskeleton-associated processes important for mediating cell motility. In this regard, human *NF2*-deficient schwannoma cells have defects in actin cytoskeleton organization that can be restored by the re-expression of wild-type, but not mutant, merlin (21). This phenotypic abnormality can also be partially rescued by modulating Rac/Rho signaling (22). In addition, regulated overexpression of wild-type merlin, but not merlin containing missense NF2 patient mutations, in rat schwannoma cells results in reduced cell motility and alterations in actin cytoskeleton organization during the initial phases of cell spreading *in vitro* (15,23).

Merlin has been shown to interact with a number of potentially important effectors, including a sodium–hydrogen exchange regulatory factor (24), an actin-binding protein (βII-spectrin) (25), schwannomin interacting protein (26), syntenin (27), the CD44 transmembrane hyaluronic acid binding protein (28,29) and hepatocyte growth factor-regulated tyrosine kinase substrate (HRS/HGS) (30,31). Merlin interacts with HRS through residues in the merlin carboxyl terminal region. Previous studies from our laboratory have shown that regulated overexpression of HRS has similar effects to overexpression of merlin on rat RT4 schwannoma cell proliferation and actin cytoskeleton-associated processes (30). HRS overexpression results in reduced RT4 cell proliferation and motility as well as alterations in actin cytoskeleton organization during the initial phases of cell spreading (31).

HRS was originally identified as a 115 kDa tyrosine-phosphorylated protein in B16-F1 mouse melanoma cells treated with hepatocyte growth factor (HGF) (32). HGF is one of the most potent mitogenic stimuli for Schwann cells and has been shown to promote cell motility in a variety of cell types (33,34). Human HRS contains 777 amino acids with several conserved protein–protein interaction domains, including a FYVE domain, a VHS zinc finger domain, a coiled-coil domain and two proline-rich regions (32). The FYVE and VHS domains have been implicated in the localization of HRS to the early endosome, where HRS functions to modulate endocytosis and exocytosis (35,36). In addition, HRS has been suggested to function in the TGF-β signaling pathway by binding to SARA, a Smad family adaptor protein (37), as well as mediate cell growth regulation by binding to the STAT signal transducing adaptor molecule (STAM) and modulating STAT pathway signaling (38).

To elucidate the relationship between HRS binding and merlin function, we determined the HRS domains required for growth suppression and merlin binding. In this report, we demonstrate that the HRS domains important for merlin binding and HRS growth suppression are distinct. We further show that merlin growth suppression is impaired in cells lacking HRS expression, but that HRS can function as a growth suppressor in the absence of merlin expression. Collectively, these results suggest that merlin growth suppression is dependent on HRS and that HRS may function to transduce the merlin growth suppressor signal.

RESULTS

Truncated HRS fragments are expressed both *in vitro* and *in vivo*

In order to study the interaction between merlin and HRS, we generated a series of truncated human HRS fragments as described in the Materials and Methods section. Truncated HRS fragments were designed to serially delete the predicted conserved protein–protein binding domains (Fig. 1A). Two approaches were taken to demonstrate HRS fragment expression. Gene expression *in vitro* was demonstrated by coupled transcription and translation *in vitro* (TNT) and proteins were detected with the 9E10 anti-myc monoclonal antibody (Fig. 1B). *In vivo* expression was demonstrated by transient transfection in RT4 schwannoma cells and detected by western blot using the 9E10 anti-myc monoclonal antibody in cell lysates (Fig. 1C). Each of the HRS fragments produced proteins of the expected sizes both *in vitro* and *in vivo*.

The merlin binding site is located within the HRS predicted coiled-coil domain

To determine the region of HRS important for mediating the interaction with merlin, we performed two complementary sets of experiments. First, we employed glutathione-*S*-transferase (GST) affinity chromatography. GST-fused carboxyl-terminal (C-term) merlin (residues 299–595) protein was used to interact with radioactive TNT products of various HRS fragments. These initial experiments demonstrated that the carboxyl terminus of merlin could interact with HRS (270–777) and HRS (447–777) as well as full-length HRS (not shown), but not with HRS (270–435) and HRS (551–777) (Fig. 2A). Further experiments showed that the carboxyl terminus of merlin also interacts with HRS (447–626) and HRS (270–550) (Fig. 2A). Based on these results, we mapped the minimal region responsible for merlin binding to HRS residues 447–550.

Second, we analysed the interaction between the carboxyl terminus of merlin and different HRS fragments *in vivo* by co-immunoprecipitation after transient transfection in RT4

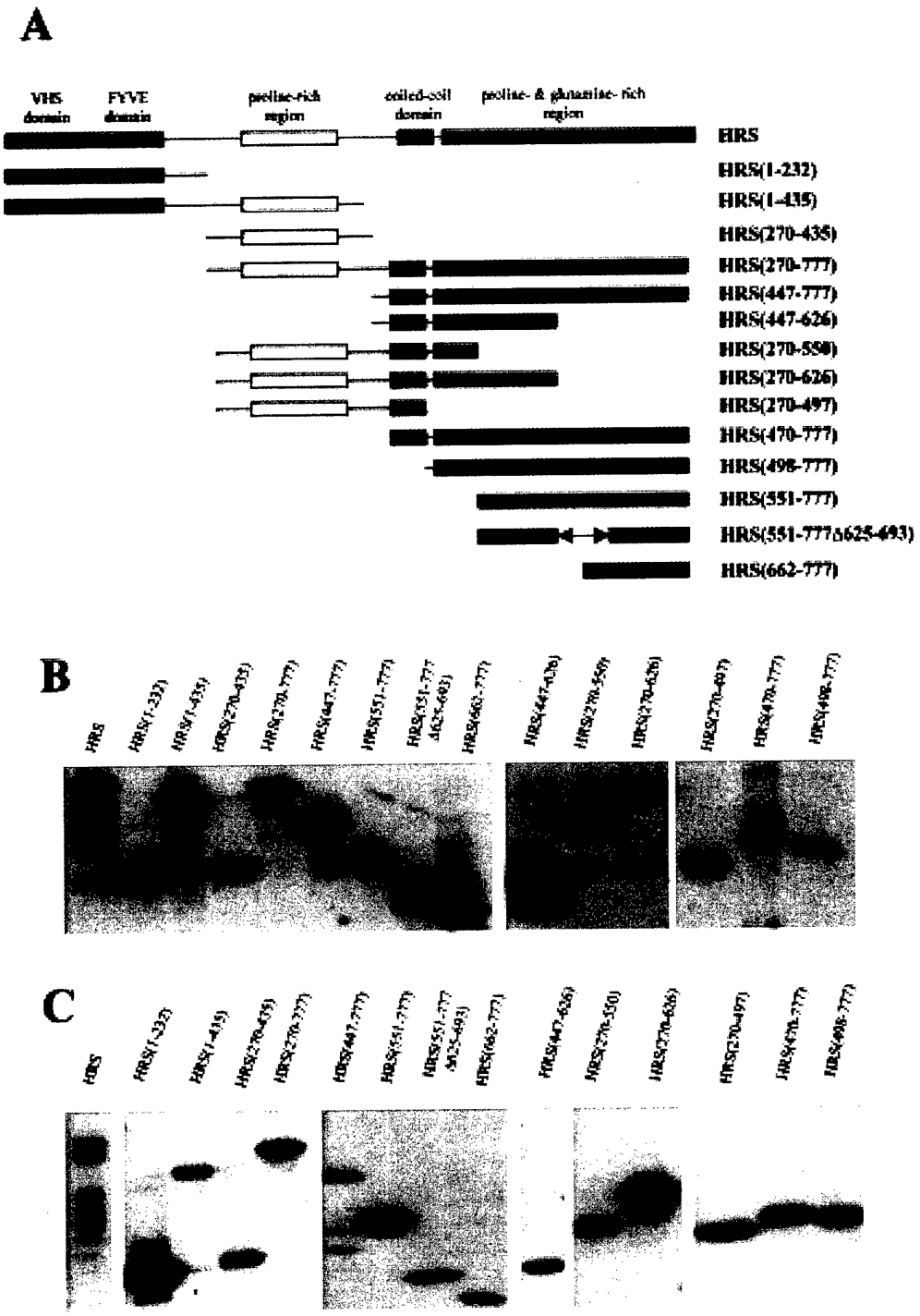

Figure 1. Generation of truncated HRS fragments. **(A)** Truncated human HRS fragments were generated by PCR to serially delete the predicted protein–protein binding domains. All fragments were cloned into the pcDNA3.myc-tagged vector. **(B)** The expression of these fragments was detected by *in vitro* transcription and translation, separation by SDS–PAGE, and western blotting with mouse anti-c-myc monoclonal antibody. **(C)** The *in vivo* expression was demonstrated by transiently transfecting fragments into RT4 rat schwannoma cells, separation by SDS–PAGE, and western blotting with c-myc antibodies.

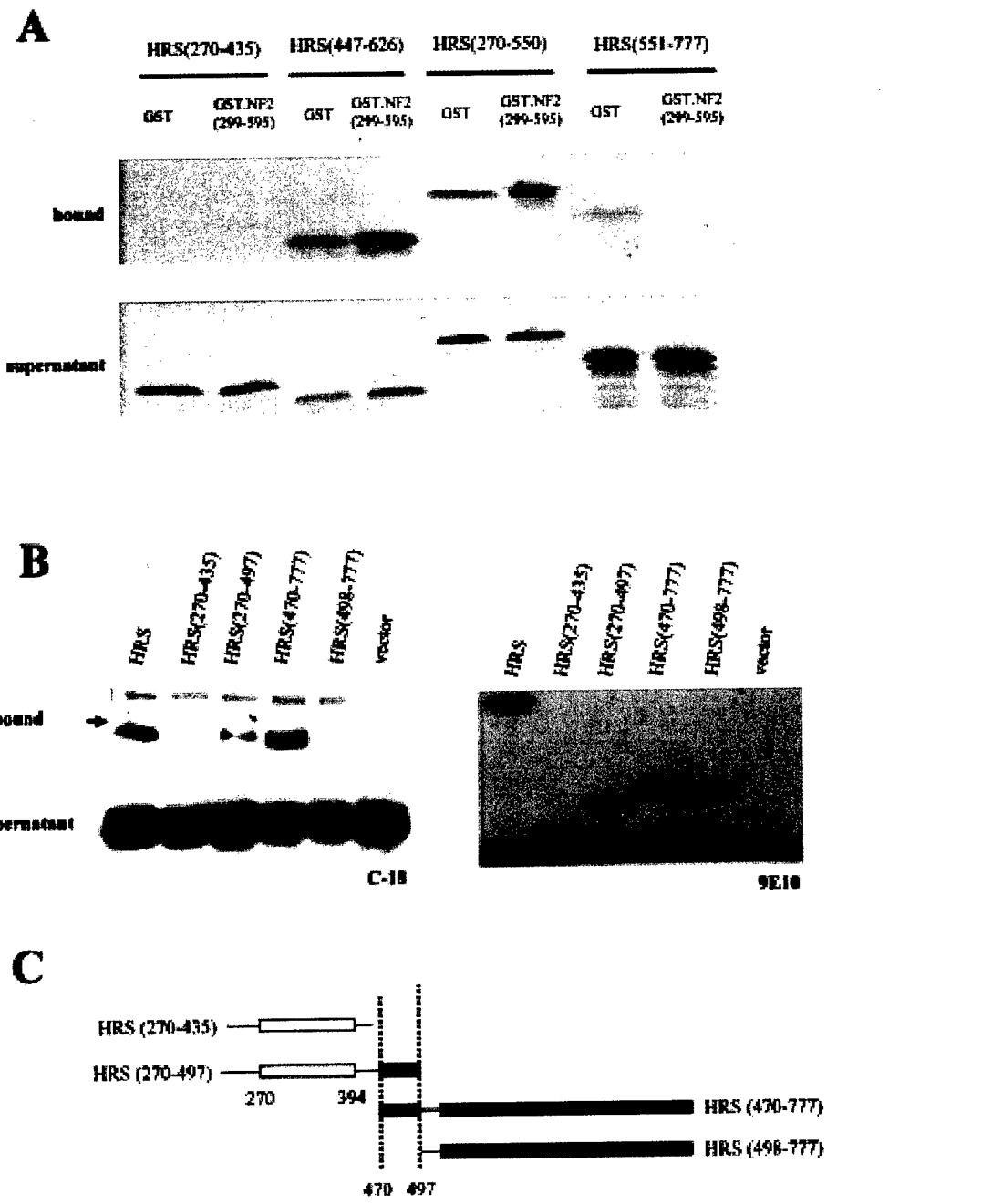

Figure 2. Merlin binding maps to the HRS coiled-coil domain. (**A**) GST-affinity chromatography experiments demonstrated that HRS (447–626) and HRS (270–550) bind to merlin (299–595), however HRS (270–435) and HRS (551–777) do not bind. (**B**) To further narrow the HRS domain that mediates binding to merlin, co-immunoprecipitation experiments were performed. The carboxyl terminus of merlin (residues 299–595) and various HRS fragments were co-transfected into RT4 cells. Cell lysates were incubated with c-myc agarose conjugate, separated by SDS–PAGE and western blotted with the C18 rabbit anti-merlin polyclonal antibody. Full length HRS, HRS (270–497) and HRS (470–777) bind to C-term merlin, but HRS (270–435) and HRS (498–777) do not, suggesting that the binding domain maps between L^{470} and R^{497}, within the HRS predicted coiled-coil domain (**C**).

cells. These experiments demonstrated that HRS (270–497) and HRS (470–777) interact with the carboxyl terminus of merlin (Fig. 2B). In other experiments, equivalent binding to the carboxyl terminus of merlin was observed with HRS (270–497) and HRS (447–777) (Fig. 4A). In contrast, HRS (270–435) and HRS (498–777) do not bind to the carboxyl terminus of merlin (Fig. 2B). Collectively, these results suggest that merlin binding to HRS required residues 470–497 within the HRS predicted coiled-coil domain (Fig. 2C).

HRS growth suppression requires residues in the carboxyl terminal domain

Next, we wanted to define the domain important for HRS growth suppression to determine whether it was distinct from the merlin-binding region. As we have shown previously, HRS overexpression results in decreased RT4 rat schwannoma cell growth in clonogenic assays as well as by using inducible RT4 cell lines (31). Using the HRS truncation constructs described above, we analysed HRS-mediated RT4 growth suppression defined as a greater than 25% reduction in colony number compared with vector controls. Initially, we observed significant HRS growth suppression with constructs HRS (270–777) and HRS (447–777) (36.53%, $P < 0.01$ and 35.35%, $P < 0.01$, respectively; Fig. 3A). In contrast, no significant growth suppression was observed with HRS (270–435) and HRS (551–777) (6.07%, $P > 0.10$ and 15.27%, $P > 0.05$, respectively; Fig. 3A). To further narrow the minimal growth suppression domain of HRS, we studied additional fragments for their ability to suppress RT4 cell growth. As shown in Figure 3B, HRS (498–777) suppressed cell growth significantly (39.7%, $P > 0.001$), while HRS (270–497) and HRS (551–777) did not (12.09%, $P > 0.05$ and 12.82%, $P > 0.05$, respectively). Growth suppression was also seen with the HRS (470–777) mutant (data not shown). Based on these experiments, the domain required for HRS growth suppression maps between residues 498 and 551, which is distinct from the sequences important for merlin binding (Fig. 3C).

A merlin-binding, but non-growth-suppressing, HRS mutant cannot reverse merlin growth suppression

Since the HRS domains important for merlin binding and HRS growth suppression were distinct and separable, we next evaluated the possibility that exogenous overexpression of an HRS fragment capable of binding to merlin, but not suppressing cell growth, might impair merlin growth suppression by interfering with endogenous merlin–HRS interactions. Using the HRS fragment containing residues 270–497, which does not suppress cell growth but binds merlin (Fig. 4A), we transfected an inducible merlin RT4 cell line with HRS (270–497) as well as other HRS truncation mutants. Whereas merlin induction using doxycycline resulted in an ~50% reduction in RT4 cell colony number ('vector'), HRS co-expression resulted in an 80% reduction (Fig. 4B and C). We observed no cooperative effect using the HRS (1–232) mutant that fails to bind merlin and lacks growth suppressor activity. HRS mutants capable of binding merlin and able to suppress growth [HRS (447–777)] exhibited similar growth suppressor properties as full length HRS. HRS (270–497) had no effect on merlin growth suppression, suggesting that interfering with endogenous merlin–HRS binding is not sufficient to reverse merlin growth suppression.

HRS is required for merlin tumor suppressor function

Given our inability to demonstrate a dominant inhibitory effect for growth suppressor defective merlin-binding mutants of HRS, we next sought to determine whether merlin growth suppression required HRS expression. To test this hypothesis, we assayed the ability of merlin to suppress cell growth in HRS-deficient mouse embryonic fibroblasts ($Hrs^{-/-}$ MEFs). The endogenous expression profiles of merlin and HRS were confirmed by Western blot using specific anti-merlin or anti-HRS antibodies (data not shown). In these experiments, merlin could not inhibit the growth of HRS deficient cells. In contrast, the re-introduction of HRS resulted in significant growth suppression (Fig. 5A). In $HRS^{+/+}$ MEF (Fig. 5B) or NIH3T3 (data not shown) cells, overexpression of either merlin or HRS resulted in growth suppression. Collectively, these data suggest that merlin growth suppression requires HRS expression.

HRS growth suppression does not require merlin expression

Since merlin cannot suppress MEF growth in the absence of HRS expression, we next wished to determine whether HRS growth suppression required merlin expression. Using *Nf2*-deficient mouse embryonic cells ($Nf2^{-/-}$ MEFs), which express endogenous HRS, we demonstrated that re-introduction of either HRS or merlin could inhibit $Nf2^{-/-}$ MEF colony formation (Fig. 5C). This is in agreement with our previous results demonstrating that HRS is capable of suppressing the growth of RT4 rat schwannoma cells that express nearly undetectable levels of merlin (31). In contrast to merlin, HRS growth suppression does not require merlin expression and suggests that HRS may function downstream of merlin in a potential growth regulatory pathway.

DISCUSSION

Among the known merlin-interacting proteins, HRS is one of the most attractive candidates for a merlin effector protein that transduces the *NF2* growth regulatory signal. Our previous studies identified HRS as a unique binding partner for merlin, which suggested that HRS might be involved in mediating merlin growth suppression (30,31). Several lines of evidence support a link between merlin and HRS. First, HRS is a specific merlin interacting protein and does not bind to other Protein 4.1 or ERM molecules (14,30). Second, HRS overexpression in RT4 rat schwannoma cells has the same functional consequences as regulated overexpression of merlin (31). Lastly, HRS functions in the HGF signaling pathway, which has been implicated in the control of Schwann cell growth and motility (33,34), processes that are also modulated by merlin (15). In this report, we define the residues on HRS required for merlin binding and HRS growth suppression and show that these regions are distinct and non-overlapping. We further

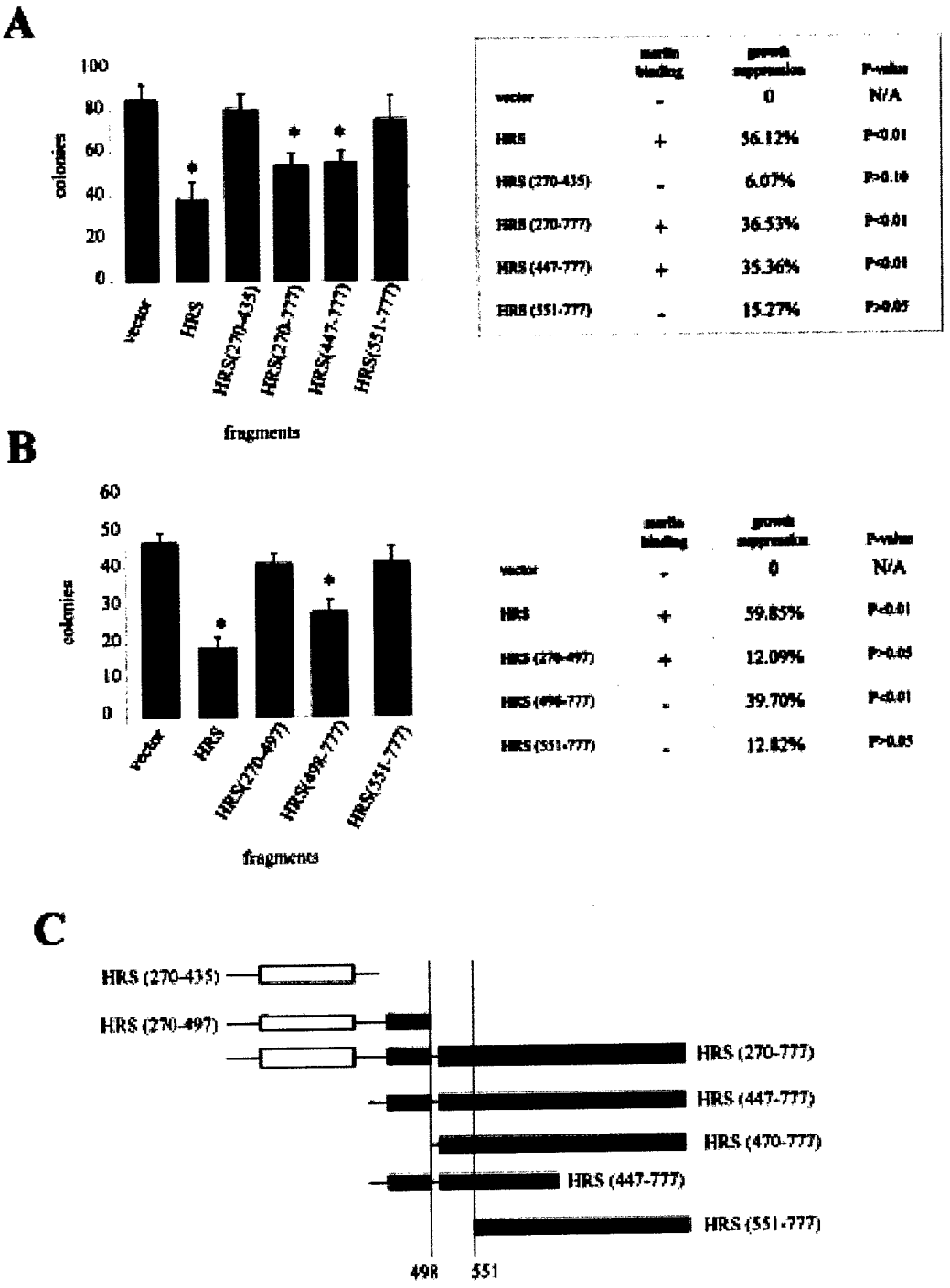

	merlin binding	growth suppression	P-value
vector	-	0	N/A
HRS	+	56.12%	P<0.01
HRS (270-435)	-	6.07%	P>0.10
HRS (270-777)	+	36.53%	P<0.01
HRS (447-777)	+	35.36%	P<0.01
HRS (551-777)	-	15.27%	P>0.05

	merlin binding	growth suppression	P-value
vector	-	0	N/A
HRS	+	59.85%	P<0.01
HRS (270-497)	+	12.09%	P>0.05
HRS (498-777)	-	39.70%	P<0.01
HRS (551-777)	-	12.82%	P>0.05

Figure 3. The carboxyl terminus of HRS is required for growth suppression. (A) In order to determine the region of HRS responsible for growth suppression, we performed clonogenic assays with various HRS fragments. HRS, HRS (270–777) and HRS (447–777) were able to suppress RT4 cell growth, whereas HRS (270–435) and HRS (551–777) did not. **(B)** Further experiments showed that HRS (498–777) also suppressed cell growth, whereas HRS (270–497) and HRS (551–777) had no effect. The growth suppressor domain of HRS maps between A^{498} and Q^{551}, which does not overlap with the merlin-binding domain (C). Asterisks denote statistically significant growth suppression.

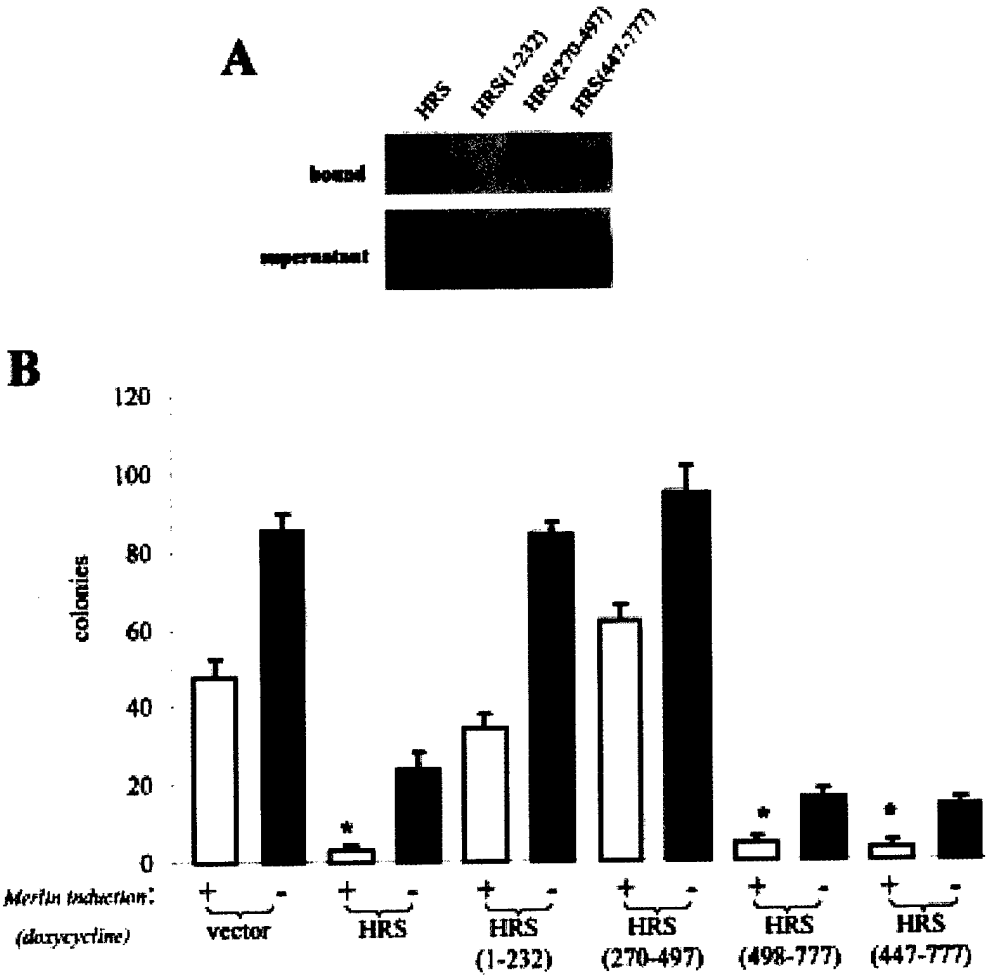

C

	Growth Suppression	Merlin Binding	merlin function	P-value
vector	-	-	52.08% ± 13.84	N/A
HRS	+	+	80.40% ± 10.08	<0.05
HRS(1-232)	-	-	51.35% ± 7.72	>0.05
HRS(270-497)	-	+	45.02% ± 12.58	>0.05
HRS(498-777)	+	-	77.82% ± 8.43	<0.05
HRS(447-777)	+	+	78.08% ± 7.87	<0.05

Figure 4. HRS (270–497) cannot reverse merlin growth suppression. (**A**) The interaction of merlin and various HRS fragments were performed by co-immunoprecipitation as described in the Materials and Methods section. Merlin interacts with HRS (270–497), HRS (447–777), as well as full-length HRS, but not HRS (1–232). (**B**) In order to determine whether expressing an HRS mutant capable of binding merlin but not reducing cell growth could inhibit merlin growth suppression, we transfected various HRS fragments into the tetracycline-regulatable RT4 rtTA NF2.17 cell line, in which merlin expression is induced upon the addition of doxycycline. In these experiments, HRS (270–497) was not able to reverse merlin growth suppression. HRS fragments with growth suppressor activity [HRS, HRS (498–777), and HRS (447–777)] cooperated with merlin to further reduce colony number. (**C**) These results are tabulated from at least four independent experiments. Asterisks denote statistically significant growth suppression.

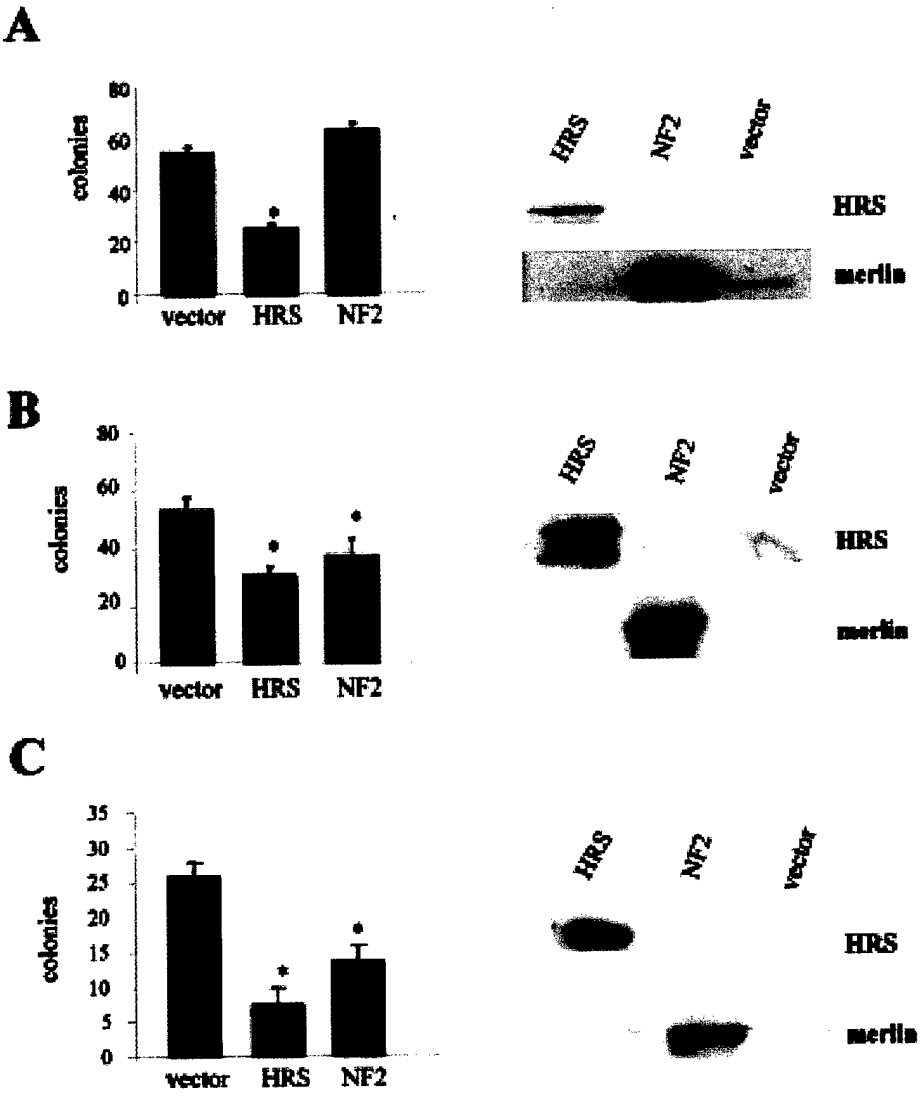

D

MEF:		$HRS^{-/-}$			$HRS^{+/+}$			$NF2^{-/-}$	
plasmid	vector	HRS	NF2	vector	HRS	NF2	vector	HRS	NF2
growth suppression (%)	0	51.68	-4.68	0	28.05	28.66	0	51.96	43.73
P-value	N/A	<0.01	>0.05	N/A	<0.05	<0.05	N/A	<0.01	<0.01

Figure 5. HRS is required for merlin growth suppression. **(A)** HRS or merlin was transiently transfected into HRS-deficient fibroblasts ($Hrs^{-/-}$ MEFs). Re-introduction of HRS into HRS deficient cells reduces cell growth, whereas merlin has no effect. The right panel shows the overexpression of HRS or merlin in HRS deficient MEFs. **(B)** Both HRS and merlin suppress $Hrs^{+/+}$ MEF growth. The right panel shows the overexpression of HRS or merlin in $Hrs^{+/+}$ MEFs. **(C)** Both HRS and merlin can suppress $Nf2^{-/-}$ MEF growth. The right panel shows the overexpression of HRS or merlin in $Nf2^{-/-}$ MEFs. The results from these experiments are tabulated in **(D)**. Asterisks denote statistically significant growth suppression.

demonstrate that merlin growth suppression requires HRS, but that HRS growth suppression is not dependent upon merlin expression. Collectively, these results suggest that HRS acts downstream of merlin and might function to transduce the merlin growth suppressor signal.

We were able to define the domain of HRS important for mediating interactions with merlin. This 'merlin-interaction' domain maps to residues 470–497 within the predicted coiled-coil domain in human HRS. A number of other HRS interacting proteins also bind to this region, including STAM (human HRS residues 452–570) (38), HRS binding protein (mouse HRS residues 431–499) (39), synaptosome-associated protein of 25 kDa (rat HRS residues 478–562) (40), p21 activated kinase 1 (human HRS residues 451–570) (41) and sorting nexin-1 (rat HRS residues 225–541) (42). Only HBP requires the same HRS binding region as merlin, based on more detailed HRS fragment binding studies. Additional mapping studies will be required to determine whether all the above HRS-binding proteins use the same binding domain as merlin. It is also not known whether HRS binding to these various molecules occurs in a mutually exclusive fashion or whether multi-molecular complexes containing a number of these proteins can exist in cells.

Using a series of HRS truncation mutants, we were able to separate the domains in HRS responsible for merlin binding from those important for growth suppression. Previously, we demonstrated that regulated overexpression of HRS dramatically reduced RT4 rat schwannoma cell proliferation and that combined HRS and merlin overexpression resulted in an additional decrease in cell growth compared with the effects of either alone (31). The domain responsible for HRS growth suppression maps to residues 498–550, which is outside of the predicted coiled-coil domain in human HRS important for merlin binding. Using a merlin inducible cell line, we now show that HRS overexpression further reduced RT4 colony number in concert with merlin overexpression. These results suggest that merlin and HRS overexpression have additive effects on growth suppression, but do not address the requirement of HRS for merlin growth suppression or vice versa. Interestingly, HRS fragments that do not bind merlin are still able to provide this additional growth suppression, arguing that HRS probably functions either downstream of or independent of merlin.

To address the requirement for HRS in merlin growth suppression, we utilized *HRS*$^{-/-}$ MEFs and demonstrated that merlin was unable to suppress cell growth in the absence of HRS expression. These results suggest that HRS functions downstream of merlin and that it is important for merlin growth suppression. In support of this downstream position, HRS growth suppression was unaffected by merlin expression and HRS was equally effective as a growth regulator in the presence or absence of merlin. Future genetic complementation studies in mice and *Drosophila* will be required to confidently position HRS and merlin function relative to each other.

Recent studies have elucidated the upstream signals that are important in merlin growth suppression. Proper membrane localization of merlin appears to be critical for merlin function, in that merlin mutants unable to associate with the cell membrane are defective as growth regulators (43,44). One such upstream molecule is the transmembrane hyaluronate receptor, CD44. Merlin binds to CD44 under growth arrest conditions (29). Under these conditions, merlin exists in a relatively hypophosphorylated form. Conversely, in the growth-permissive state, merlin is hyperphosphorylated and exhibits decreased binding to CD44. In this model (45), merlin growth suppression occurs in a specific cellular context and its association with CD44 is partially mediated by phosphorylation events (46,47). Another 'upstream' merlin interacting protein is paxillin, which binds to merlin and regulates its density-dependent localization (48). Paxillin binds to merlin residues 50–70 contained within exon 2 and facilitates the localization of merlin to the cell membrane where it can interact with cell surface proteins, like CD44 and β1-integrin (49).

While these studies shed light on the upstream signaling events relevant to merlin growth suppression, comparatively less is known about the pathways and events downstream of merlin that transduce the merlin growth suppressor signal. A number of potential interacting proteins have been identified over the years since the cloning of the *NF2* gene. Some of these molecules also bind other ERM proteins (e.g. βII-spectrin) (25), while others have unknown functions (e.g. schwannomin-interacting protein) (26). One interesting merlin interactor that operates within a critical Schwann cell signaling pathway is HRS. Our results positioning HRS downstream of merlin in mammalian cells suggest that HRS may transduce merlin growth suppression. Several possibilities can be envisioned to explain how HRS might propagate merlin's signal. First, merlin may serve to bring HRS to the cell membrane where it can interact with key molecules. We examined the possibility that merlin overexpression might serve to redistribute HRS within cells. In these experiments, we observed no change in HRS subcellular distribution upon merlin induction (C.X.S., unpublished observations). Similarly, we did not see any change in merlin subcellular localization upon HRS overexpression. These results argue that this mechanism is unlikely to explain how HRS functions as a merlin signal transducer. Further studies will be required to determine whether HRS changes the ability of merlin to interact with specific cell membrane proteins.

Alternatively, merlin could bind to HRS and result in activation of HRS by facilitating its interaction with specific HRS effector proteins. While HRS growth suppression is not dependent upon merlin expression, merlin binding to HRS may allow HRS to function more efficiently as a negative growth regulator. In this fashion, merlin-mediated HRS activation would lead to decreased cell growth, perhaps by modulating pathways previously ascribed to HRS, such as endocytosis and exocytosis (50–57), lysosomal trafficking (42), TGF-β:Smad signaling (37), or Jun kinase (JNK) activation (38). The role of HRS in JNK activation is particularly intriguing in light of experiments demonstrating increased JNK signaling in *Nf2*$^{-/-}$ mouse embryonic fibroblasts (46). In addition, recent studies have indicated that HRS might participate in receptor tyrosine kinase (RTK) endocytosis (52). In this model, HRS activation might modulate the endocytosis of RTK molecules (36,39,53), like epidermal or hepatocyte growth factor receptor, to affect mitogenic signaling and cell proliferation. Additional studies will be necessary to dissect the mechanism(s) underlying HRS-dependent merlin growth regulation.

MATERIALS AND METHODS

Antibodies, plasmids, and cell lines

The merlin and HRS cDNAs used in these experiments were of human origin as described previously (30,31). HRS fragments were generated with PCR. The primers for PCR are: HRS (1–232), 5′-CTG GAT CCC GGG CGA GGC AGC GGC ACC-3′ and 5′-CTC ACT CAG TGG TGG AAG TGG C-3′; HRS (1–435), 5′-CTG GAT CCC GGG CGA GGC AGC GGC ACC-3′ and 5′-CTC AAC TCT TCA TGC GGT TCA C-3′; HRS (270–435), 5′-CTG GAT CCC CAG TCA GAG GCG GAG GAG-3′ and 5′-CTC AAC TCT TCA TGC GGT TCA C-3′; HRS (270–777), 5′-CTG GAT CCC CAG TCA GAG GCG GAG GAG-3′ and 5′-GTC AGT CGA ATG AAA TGA GCT G-3′; HRS (447–777), 5′-CTG GAT CCC AAC GGC ATG CAC CCG CAG-3′ and 5′-GTC AGT CGA ATG AAA TGA GCT G-3′; HRS (447–626), 5′-CTG GAT CCC AAC GGC ATG CAC CCG CAG-3′ and 5′-CTC ACG CAG TGC TGG GCA TGC T-3′; HRS (270–550), 5′-CTG GAT CCC CAG TCA GAG GCG GAG GAG-3′ and 5′-GTC ACT GCT GCT CCA GCC GCA TC-3′; HRS (270–626), 5′-CTG GAT CCC CAG TCA GAG GCG GAG GAG-3′ and 5′-CTC ACG CAG TGC TGG GCA TGC T-3′; HRS (270–497), 5′-CTG GAT CCC CAG TCA GAG GCG GAG GAG-3′ and 5′-GTC ACC GGC GAA GCT TCT CCC GGT G-3′; HRS (470–777), 5′-CTG GAT CCC CTG CAG GAC AAG CTG GCA C-3′ and 5′-GTC AGT CGA ATG AAA TGA GCT G-3′; HRS (498–777), 5′-CTG GAT CCC GCA GCC GAG GAG GCA GAG C-3′ and 5′-GTC AGT CGA ATG AAA TGA GCT G-3′; HRS (551–777), 5′-CTG GAT CCC AAG CAG ACG GTC CAG ATG C-3′ and 5′-GTC AGT CGA ATG AAA TGA GCT G-3′; HRS (551–777Δ625–693), 5′-CTG GAT CCC AAG CAG ACG GTC CAG ATG C-3′ and 5′-GTC AGT CGA ATG AAA TGA GCT G-3′; HRS (662–777), 5′-CTG GAT CCC TCC TAC CAG CCT ACT CCC ACA-3′ and 5′-GTC AGT CGA ATG AAA TGA GCT G-3′ . PCR products containing a *Bam*HI restriction site were initially cloned into pCR2.1 T/A cloning vector (Invitrogen Inc.) and sequenced in their entirety. HRS fragments were next subcloned into a pcDNA3.myc vector generated in our laboratory.

Mouse anti-myc monoclonal antibody (9E10), mouse anti-myc monoclonal antibody agarose conjugates (9E10 AC) and rabbit anti-merlin polyclonal antibody (C18 and A19) were purchased from Santa Cruz Technology. Rabbit anti-HRS polyclonal antibody (Ab10802) was generated as described previously (30). Tubulin (clone DM1A) was purchased from Sigma (St Louis, MO, USA).

The RT4 rat schwannoma cell line was maintained in complete DMEM with 10% FBS. Mouse embryonic fibroblasts ($Hrs^{-/-}$; $Hrs^{+/+}$ and $Nf2^{+/+}$) and NIH3T3 cells were maintained in complete DMEM with 10% FBS. *NF2*-deficient ($Nf2^{-/-}$) MEFs were provided by Dr Marco Giovannini (Fondation Jean Dausset, CEPH, France) and maintained in complete DMEM plus 10% FBS and 0.1 mM β-mercaptoethanol. The merlin inducible rtTA.merlin RT4 cells were maintained in complete DMEM with 10% FBS, selected by 500 μg/ml G418, and 1 μg/ml puromycin. Merlin expression was induced by addition of 1 μg/ml doxycycline.

In vitro and *in vivo* protein expression

To determine the expression of constructed HRS fragments *in vitro*, a nonradioactive coupled transcription/translation reaction was performed using the TNT® coupled Reticulocyte Lysate System (Promega) according to the recommended protocol. Nonradioactive products were separated by 12% SDS–PAGE and analysed by western blot using the 9E10 myc monoclonal antibody. To analyse the expression of truncated HRS fragments *in vivo*, RT4 cells were seeded in six-well plates and transfected with various HRS fragments using Lipofectamine according to the manufacturer's recommendations. Cell lysates were harvested 48 h later, separated by SDS–PAGE and analysed by western blot using the 9E10 myc antibody.

Growth suppression assay

Clonogenic assays were performed by transfecting cells with equimolar amounts of vector (pcDNA3.myc), pcDNA3.myc.HRS and various HRS fragments in pcDNA3.myc vector. Cells were selected in 500 μg/ml G418 for 14 days and the number of surviving colonies greater than 1 mm were counted in quadruplicate dishes after staining in 0.5% Crystal violet. In some experiments, transfected cells were selected in 500 μg/ml G418, 1 μg/ml puromycin and 200 μg/ml hygromycin. Merlin induction in rtTA.merlin RT4 cells lines was accomplished using 1 μg/ml doxycycline, as previously reported (15). Each experiment was repeated at least three times with identical results.

To determine merlin or HRS function in genetically-defined MEFs, we transiently transfected equimolar amounts of vector (pcDNA3), pcDNA3.HRS, or pcDNA3.NF2 plus 10-fold less pBABE.PURO plasmid. Cells were selected by 1 μg/ml puromycin for 14 days, and surviving colonies were counted as above. Each experiment was repeated for four times with identical results.

GST protein affinity chromatography

Glutathione-*S*-transferase (GST)–merlin fusion proteins were generated as previously described (13,58). Briefly, GST.C-term merlin (residues 299–595) was transformed into DE3 (BL21) competent cells for fusion protein production. Bacteria were induced in 0.4 mM IPTG at room temperature for 20–21 hrs and GST fusion protein was collected on glutathione–agarose beads (Sigma) for the interaction experiments.

GST fusion protein was prepared as above for HRS–merlin interaction experiments with *in vitro* transcribed and translated HRS fragment proteins. *In vitro* transcribed and translated HRS fragment proteins were synthesized in the presence of [^{35}S]-methionine using the TNT® coupled Reticulocyte Lysate Systems (Promega) and detected by autoradiography. In these experiments, radiolabeled proteins were incubated with equimolar amounts of GST fusion protein immobilized on glutathione–agarose beads for 4 h at 4°C. Supernatants were saved and the beads were washed three times with TEN buffer (10 mM Tris–Cl pH 7.5, 150 mM NaCl, 5 mM EDTA, 1% Triton X-100) and eluted in 2× Laemmli buffer. Supernatants and eluted bound fractions were separated by 12% SDS–PAGE and

analysed by autoradiography. Each interaction experiment was repeated at least three times with identical results.

In vivo HRS interaction experiments

RT4 schwannoma cells were transiently transfected with merlin constructs and various HRS fragments using LipofectAMINE (Gibco BRL) and lysates prepared 48 h later using NP-40 lysis buffer (50 mM Tris, pH 7.4; 150 mM NaCl; 3 mM $MgCl_2$; 0.5% NP 40; 1 mM DTT; 1 mM PMSF; 10 μg/ml aprotinin; 10μg/ml leupeptin). Protein lysates were incubated with the myc antibody conjugated to agarose beads (Santa Cruz Biotechnology) for 2 h at 4°C followed by extensive washing with 1× PBS. Eluted proteins were separated by SDS–PAGE and blotted with the C18 anti-merlin polyclonal antibody to detect merlin proteins. Membranes were probed with the 9E10 myc antibody after stripping with ECL stripping buffer (6.25 ml 1 M Tris, pH 6.8; 770 μl β-mercaptoethanol; 10 ml 20% SDS; ddH_2O to 100 ml). Each experiment was repeated at least three times with identical results.

ACKNOWLEDGEMENTS

We thank the members of our laboratory for their expert assistance during the execution of this project. These studies were supported by a grant from the National Institutes of Health (NS35848 to D.H.G.).

REFERENCES

1. Evans, D.G., Huson, S.M., Donnai, D., Neary, W., Blair, V., Newton, V., Strachan, T. and Harris, R. (1992) A genetic study of type 2 neurofibromatosis in the United Kingdom. II. Guidelines for genetic counseling. *J. Med. Genet.*, **29**, 847–852.
2. Rouleau, G.A., Merel, P., Lutchman, M., Sanson, M., Zucman, J., Marineau, C., Xuan, K.H., Demczuk, S., Desmaze, C., Plougastel, B. *et al.* (1993) Alteration in a new gene coding a putative membrane-organizing protein causes neuro-fibromatosis type 2. *Nature*, **363**, 515–521.
3. Trofatter, J.A., MacCollin, M.M., Rutter, J.L., Murrell, J.R., Duyao, M.P., Parry, D.M., Eldridge, R., Kley, N., Menon, A., Pulaski, K. *et al.* (1993) A novel moesin-, ezrin-, radixin-like gene is a candidate for the neurofibromatosis 2 tumor suppressor. *Cell*, **72**, 791–800
4. Tsukita, S., Yonemura, S. and Tsukita, S. (1997) ERM family: from cytoskeleton to signal transduction. *Curr. Opin. Cell Biol.*, **9**, 70–75.
5. Gautreau, A., Poullet, P., Louvard, D., Arpin, M. (1999) Ezrin, a plasma membrane–microfilament linker, signals cell survival through the phosphatidylinositol 3-kinase/Akt pathway. *Proc. Natl Acad. Sci. USA*, **96**, 7300–7305.
6. Xu, H.M. and Gutmann, D.H. (1998) Merlin differentially associates with the microtubule and actin cytoskeleton. *J. Neurosci. Res.*, **51**, 403–415.
7. Scherer, S.S. and Gutmann, D.H. (1996) Expression of the neurofibromatosis 2 tumor suppressor gene product, merlin, in Schwann cells. *J. Neurosci. Res.*, **46**, 595–605.
8. Scherer, S.S., Xu, T., Crino, P., Arroyo, E.J. and Gutmann, D.H. (2001) Ezrin, radixin, and moesin are components of Schwann cell microvilli. *J. Neurosci. Res.*, **65**, 150–164.
9. Gutmann, D.H. (2001) The neurofibromatoses: when less is more. *Hum. Mol. Genet.*, **10**, 747–755.
10. Sainz, J., Huynh, D.P., Figueroa, K., Ragge, N.K., Baser, M.E. and Pulst, S.M. (1994) Mutations of the neurofibromatosis type 2 gene and lack of the gene product in vestibular schwannomas. *Hum. Mol. Genet.*, **3**, 885–891.
11. Bourn, D., Carter, S.A., Mason, S., Gareth, D., Evans, R. and Strachan, T. (1994) Germline mutations in the neurofibromatosis type 2 tumour suppressor gene. *Hum. Mol. Genet.*, **3**, 813–816.
12. Huynh, D.P., Mautner, V., Baser, M.E., Stavrou, D. and Pulst, S.M. (1997) Immunohistochemical detection of schwannomin and neurofibromin in vestibular schwannomas, ependymomas and meningiomas. *J. Neuropathol. Exp. Neurol.*, **56**, 382–390.
13. Sherman, L., Xu, H.-M., Geist, R.T., Saporito-Irwin, S., Howells, N., Ponta, H., Herrlich, P. and Gutmann, D.H. (1997) Interdomain binding mediates tumor growth suppression by the NF2 gene product. *Oncogene*, **15**, 2505–2509.
14. Gutmann, D.H., Hirbe, A.C., Huang, Z.Y. and Haipek, C.A. (2001) The protein 4.1 tumor suppressor, DAL-1, impairs cell motility, but regulates proliferation in a cell-type-specific fashion. *Neurobiol. Dis.*, **8**, 266–278.
15. Gutmann, D.H., Hirbe, A.C. and Haipek, C.A. (2001) Functional analysis of neurofibromatosis 2 (NF2) missense mutations. *Hum. Mol. Genet.*, **10**, 1519–1529.
16. Ruttledge, M.H., Sarrazin, J., Rangaratnam, S., Phelan, C.M., Twist, E., Merel, P., Delattre, O., Thomas, G., Nordenskjöld, M. *et al.* (1994) Evidence for the complete inactivation of the NF2 gene in the majority of sporadic meningiomas. *Nat. Genet.*, **6**, 180–184.
17. Gutmann, D.H., Giordano, M.J., Fishback, A.S. and Guha, A. (1997) Loss of merlin expression in sporadic meningiomas, ependymomas and schwannomas. *Neurology*, **49**, 267–270.
18. Stemmer-Rachamimov, A.O., Gonzalez-Agosti, C., Xu, L., Burwick, J.A., Beauchamp, R., Pinney, D., Louis, D.N. and Ramesh, V. (1997) Expression of NF2-encoded merlin and related ERM family proteins in the human central nervous system. *J. Neuropath Exp Neurol.*, **56**, 735–742.
19. Deprez, R.H.L., Bianchi, A.B., Groen, N.A., Seizinger, B.R., Hagemeijer, A., van Drunen, E., Bootsma, D., Koper, J.W., Avezaat, C.J.J., Kley, N. and Zwarthoff, E.C. (1994) Frequent NF2 gene transcript mutations in sporadic meningiomas and vestibular schwannomas. *Am. J. Hum. Genet.*, **54**, 1022–1029.
20. McClatchey, A.I., Saotome, I., Mercer, K., Crowley, D., Gusella, J.F., Bronson, R.T. and Jacks, T. (1998) Mice heterozygous for a mutation at the Nf2 tumor suppressor locus develop a range of highly metastatic tumors. *Genes Devl.*, **12**, 1121–1133.
21. Bashour, A.M., Meng, J.J., Ip, W., MacCollin, M. and Ratner, N. (2002) The neurofibromatosis type 2 gene product, merlin, reverses the F-actin cytoskeletal defects in primary human Schwannoma cells. *Mol. Cell Biol.*, **22**, 1150–1157.
22. Pelton, P.D., Sherman, L.S., Rizvi, T.A., Marchionni, M.A., Wood, P., Friedman, R.A. and Ratner, N. (1998) Ruffling membrane, stress fiber, cell spreading, and proliferation abnormalities in human schwannoma cells. *Oncogene*, **17**, 2195–2209.
23. Gutmann, D.H., Sherman, L., Seftor, L., Haipek, C., Hoang, Lu, K. and Hendrix, M. (1999) Increased expression of the NF2 tumor suppressor gene product, merlin, impairs cell motility, adhesion and spreading. *Hum. Mol. Genet.*, **8**, 267–275.
24. Murthy, A., Gonzalez-Agosti, C., Cordero, E., Pinney, D., Candia, C., Solomon, F., Gusella, J. and Ramesh, V. (1998) NHE-RF, a regulatory cofactor for Na(+)–H(+) exchange, is a common interactor for merlin and ERM (MERM) proteins. *J. Biol. Chem.*, **273**, 1273–1276.
25. Scoles, D.R., Huynh, D.P., Morcos, P.A., Coulsell, E.R., Robinson, N.G., Tamanoi, F. and Pulst, S.M. (1998) Neurofibromatosis 2 tumour suppressor schwannomin interacts with βII-spectrin. *Nat. Genet.*, **18**, 354–359.
26. Goutebroze, L., Brault, E., Muchardt, C., Camonis, J. and Thomas, G. (2000) Cloning and characterization of SCHIP-1, a novel protein interacting specifically with spliced isoforms and naturally occurring mutant NF2 proteins. *Mol. Cell Biol.*, **20**, 1699–1712.
27. Jannatipour, M., Dion, P., Khan, S., Jindal, H., Fan, X., Laganiere, J., Chishti, A.H. and Rouleau, G.A. (2001) Schwannomin isoform-1 interacts with syntenin via PDZ domains. *J. Biol. Chem.*, **276**, 33093–33100.
28. Sainio, M., Zhao, F., Heiska, L., Turunen, O., den Bakker, M., Zwarthoff, E., Lutchman, M., Rouleau, G.A., Jaaskelainen, J., Vaheri, A. and Carpen, O. (1997) Neurofibromatosis 2 tumor suppressor protein colocalizes with ezrin and CD44 and associates with actin-containing cytoskeleton. *J. Cell Sci.*, **110**, 2249–2260.
29. Morrison, H., Sherman, L.S., Legg, J., Banine, F., Isacke, C., Haipek, C.A., Gutmann, D.H., Ponta, H. and Herrlich, P. (2001) The NF2 tumor suppressor gene product, merlin, mediates contact inhibition of growth through interactions with CD44. *Genes Devl.*, **15**, 968–980.
30. Scoles, D.R., Huynh, D.P., Chen, M.S., Burke, S.P., Gutmann, D.H. and Pulst, S.M. (2000) The neurofibromatosis 2 tumor suppressor protein interacts with hepatocyte growth factor-regulated tyrosine kinase substrate. *Hum. Mol. Genet.*, **9**, 1567–1574.

31. Gutmann, D.H., Haipek, C.A., Burke, S.P., Sun, C.X., Scoles, D.R. and Pulst, S.M. (2001) The NF2 interactor, hepatocyte growth factor-regulated tyrosine kinase substrate (HRS), associates with merlin in the "open" conformation and suppresses cell growth and motility. *Hum. Mol. Genet.*, **10**, 825–834.
32. Komada, M. and Kitamura, N. (1995) Growth factor-induced tyrosine phosphorylation of Hrs, a novel 115-kilodalton protein with a structurally conserved putative zinc finger domain. *Mol. Cell Biol.*, **15**, 6213–6121.
33. Krasnoselsky, A., Massay, M.J., DeFrances, M.C., Michalopoulos, G., Zarnegar, R. and Ratner, N. (1994) Hepatocyte growth factor is a mitogen for Schwann cells and is present in neurofibromas. *J. Neurosci.*, **14**, 7284–7290.
34. Maulik, G., Shrikhande, A., Kijima, T., Ma, P.C., Morrison, P.T. and Salgia, R. (2002) Role of the hepatocyte growth factor receptor, c-Met, in oncogenesis and potential for therapeutic inhibition. *Cytokine Growth Factor Rev.*, **13**, 41–59.
35. Komada, M. and Soriano, P. (1999) Hrs, a FYVE finger protein localized to early endosomes, is implicated in vesicular traffic and required for ventral folding morphogenesis. *Genes Devl.*, **13**, 1475–1485.
36. Mao, Y., Nickitenko, A., Duan, X., Lloyd, T.E., Wu, M.N., Bellen, H. and Quiocho, F.A. (2000) Crystal structure of the VHS and FYVE tandem domains of Hrs, a protein involved in membrane trafficking and signal transduction. *Cell*, **100**, 447–456.
37. Miura, S., Takeshita, T., Asao, H., Kimura, Y., Murata, K., Sasaki, Y., Hanai, J.I., Beppu, H., Tsukazaki, T., Wrana, J.L. *et al.* (2000) Hgs (Hrs), a FYVE domain protein, is involved in Smad signaling through cooperation with SARA. *Mol. Cell Biol.*, **20**, 9346–9355.
38. Asao, H., Sasaki, Y., Arita, T., Tanaka, N., Endo, K., Kasai, H., Takeshita, T., Endo, Y., Fujita, T. and Sugamura, K. (1997) Hrs is associated with STAM, a signal-transducing adaptor molecule. Its suppressive effect on cytokine-induced cell growth. *J. Biol. Chem.*, **272**, 32785–32791.
39. Takata, H., Kato, M., Denda, K. and Kitamura, N. (2000) A hrs binding protein having a Src homology 3 domain is involved in intracellular degradation of growth factors and their receptors. *Genes Cells*, **5**, 57–69.
40. Kwong, J., Roundabush, F.L., Hutton Moore, P., Montague, M., Oldham, W., Li, Y., Chin, L.S. and Li, L. (2000) Hrs interacts with SNAP-25 and regulates Ca(2+)-dependent exocytosis. *J. Cell Sci.*, **113**, 2273–2284.
41. Sasaki, Y. and Sugamura, K. (2001) Involvement of Hgs/Hrs in signaling for cytokine-mediated c-fos induction through interaction with TAK1 and Pak1. *J. Biol. Chem.*, **276**, 29943–29952.
42. Chin, L.S., Raynor, M.C., Wei, X., Chen, H.Q. and Li, L. (2001) Hrs interacts with sorting nexin 1 and regulates degradation of epidermal growth factor receptor. *J. Biol. Chem.*, **276**, 7069–7078.
43. Brault, E., Gautreau, A., Lamarine, M., Callebaut, I., Thomas, G. and Goutebroze, L. (2001) Normal membrane localization and actin association of the NF2 tumor suppressor protein are dependent on folding of its N-terminal domain. *J. Cell Sci.*, **114**, 1901–1912.
44. Schulze, K.M., Hanemann, C.O., Muller, H.W. and Hanenberg, H. (2002) Transduction of wild-type merlin into human schwannoma cells decreases schwannoma cell growth and induces apoptosis. *Hum. Mol. Genet.*, **11**, 69–76.
45. Sherman, L.S. and Gutmann, D.H. (2001) Merlin: hanging tumor suppression on the Rac. *Trends Cell Biol.*, **11**, 442–444.
46. Shaw, R.J., Paez, J.G., Curto, M., Yaktine, A., Pruitt, W.M., Saotome, I., O'Bryan, J.P., Gupta, V., Ratner, N., Der, C.J. *et al.* (2001) The Nf2 tumor suppressor, merlin, functions in Rac-dependent signaling. *Devl. Cell*, **1**, 63–72.
47. Xiao, G.H., Beeser, A., Chernoff, J. and Testa, J.R. (2002) p21-activated kinase links Rac/Cdc42 signaling to merlin. *J. Biol. Chem.*, **277**, 883–886.
48. Fernandez-Valle, C., Tang, Y., Ricard, J., Rodenas-Ruano, A., Taylor, A., Hackler, E., Biggerstaff, J. and Iacovelli, J. (2002) Paxillin binds schwannomin and regulates its density-dependent localization and effect on cell morphology. *Nat. Genet.*, **31**, 354–362.
49. Obremski, V.J., Hall, A.M. and Fernandez-Valle, C. (1998) Merlin, the neurofibromatosis type 2 gene product, and beta1 integrin associate in isolated and differentiating Schwann cells. *J. Neurobiol.*, **37**, 487–501.
50. Komada, M. and Kitamura, N. (2001) Hrs and hbp: possible regulators of endocytosis and exocytosis. *Biochem. Biophys. Res. Commun.*, **281**, 1065–1069.
51. Raiborg, C., Bache, K.G., Gillooly, D.J., Madshus, I.H., Stang, E. and Stenmark, H. (2002) Hrs sorts ubiquitinated proteins into clathrin-coated microdomains of early endosomes. *Nat. Cell Biol.*, **4**, 394–398.
52. Raiborg, C., Bache, K.G., Mehlum, A. and Stenmark, H. (2001) Function of Hrs in endocytic trafficking and signalling. *Biochem. Soc. Trans.*, **29**, 472–475.
53. Lloyd, T.E., Atkinson, R., Wu, M.N., Zhou, Y., Pennetta, G. and Bellen, H.J. (2002) Hrs regulates endosome membrane invagination and tyrosine kinase receptor signaling in *Drosophila*. *Cell*, **108**, 261–269.
54. Li, Y., Chin, L.S., Levey, A.I. and Li, L. (2002) Huntingtin-associated protein 1 interacts with Hrs and functions in endosomal trafficking. *J. Biol. Chem.* [epub ahead of print].
55. Raiborg, C., Bache, K.G., Mehlum, A., Stang, E. and Stenmark, H. (2001) Hrs recruits clathrin to early endosomes. *EMBO J.*, **20**, 5008–5021.
56. Murai, S. and Kitamura, N. (2000) Involvement of hrs binding protein in IgE receptor-triggered exocytosis in RBL-2H3 mast cells. *Biochem. Biophys. Res. Commun.*, **277**, 752–756.
57. Urbe, S., Mills, I.G., Stenmark, H., Kitamura, N. and Clague, M.J. (2000) Endosomal localization and receptor dynamics determine tyrosine phosphorylation of hepatocyte growth factor-regulated tyrosine kinase substrate. *Mol. Cell Biol.*, **20**, 7685–7692.
58. Gutmann, D.H., Geist, R.T., Xu, H., Kim, J.S. and Saporito-Irwin, S. (1998) Defects in neurofibromatosis 2 protein function can arise at multiple levels. *Hum. Mol. Genet.*, **7**, 335–345.

Biochemical and Biophysical Research Communications **290,** 366–374 (2002)
doi:10.1006/bbrc.2001.6178, available online at http://www.idealibrary.com on IDEAL®

Effects of *Nf2* Missense Mutations on Schwannomin Interactions

Daniel R. Scoles,[1] Mercy Chen, and Stefan-M. Pulst

Neurogenetics Laboratory and Division of Neurology, CSMC Burns and Allen Research Institute, Cedars-Sinai Medical Center, School of Medicine, University of California at Los Angeles, 8700 Beverly Boulevard, Los Angeles, California 90048

Received November 15, 2001

Most benign brain tumors are associated with loss of the *Nf2* gene tumor suppressor product schwannomin/merlin. Interactions between schwannomin fragments have given rise to hypotheses of *in vivo* schwannomin folding and dimerization. Previously, we showed that schwannomin with missense mutations L360P, L535P, and Q538P alters interaction with βII-spectrin and Hrs. Using yeast two-hybrid tests of interaction, we now show the effects of 11 *Nf2* missense mutations on schwannomin self-interaction as well as schwannomin interaction with Hrs isoforms 1 and 2, βII-spectrin, and p110. Missense mutations L46R and K364I significantly decreased affinity of schwannomin for binding all interacting proteins. The schwannomin L46R mutation may result in a complex conformational change that alters folding and denies βII-spectrin access to an intact binding site in the C-terminal half of schwannomin. We show that unique inter- and intramolecular interactions occur for schwannomin isoform 2, suggesting that this schwannomin isoform has unique functional properties compared to schwannomin isoform 1. © 2002 Elsevier Science

Key Words: **neurofibromatosis; NF2; schwannomin; merlin; βII-spectrin; Hrs; p110; missense; mutation.**

Neurofibromatosis 2 (NF2) is an autosomal dominant disorder characterized by benign tumors of the neural crest. The *Nf2* gene is commonly mutated in benign tumors of the human nervous system, including nearly all vestibular schwannomas, most sporadic meningiomas and some ependymomas (1–5). Familial NF2 is also characterized by a variety of nontumor features in addition to tumors, including cataracts, retinal hamartomas, and café-au-lait spots (6).

[1] To whom correspondence and reprint requests should be addressed at Division of Neurology, Cedars-Sinai Medical Center, 1145E Medical Tower, 8631 West 3rd Street, Los Angeles, CA 90048. Fax: (310) 423-0149. E-mail: scolesd@cshs.org.

The *Nf2* gene product schwannomin (SCH), also named merlin, is a tumor suppressor whose biochemical actions are not fully understood. SCH has high homology with ezrin, radixin, and moesin (ERM proteins) of the protein 4.1 superfamily that link the cytoskeleton to the plasma membrane (7, 8). Schwannomin occurs in two predominant isoforms, SCHi1 and SCHi2. Alternative splicing of *Nf2* exon 16, which encodes an alternative termination codon, results in the replacement of the last 16 amino acids (aa) encoded by exon 17 of SCHi1 (595 aa) with 11 aa of SCHi2 (590 aa) (9, 10).

Binding sites in the SCH N-terminal domain can be masked by conformational changes, similar to the binding site masking that occurs in ERM proteins (11, 12). This is interesting in the context that missense or truncating *Nf2* mutations may alter conformation resulting in unmasking or further masking of binding sites on schwannomin. Unfolding of ezrin unmasks an N-terminal domain binding site for the ezrin binding phosphoprotein EBP50 (13), and a C-terminal domain binding site for F-actin (14). In schwannomin, tubulin binding sites in the N-terminal domain are masked in full-length protein (15). In addition, interaction tests using the yeast two-hybrid method showed full-length SCH binds N- and C-terminal SCH fragments but not N- and C-terminal ezrin fragments unless SCH is truncated (16). This suggested that homodimerization sites on SCH are exposed while the binding sites for ezrin on SCH are masked (16). Thus full-length SCH possesses masked tubulin binding sites in the N-terminal domain, as well as masked binding sites for ezrin that are likely unique from the SCH homodimerization sites.

While efforts have been made to demonstrate the effects of schwannomin truncation on schwannomin interactions, little information is available on the effects of natural *Nf2* missense mutations on schwannomin interactions. Previously we identified the HGF-regulated tyrosine kinase substrate (HRS) isoform 1 (HRSi1), HRS isoform 2 (HRSi2) (17), βII-spectrin (18), and the eukaryotic initiation factor 3 (eIF3) p110 sub-

0006-291X/02 $35.00

unit eight (Scoles and Pulst, in preparation) as schwannomin interacting proteins. Each of HRSi1, HRSi2, and βII-spectrin interact with the C-terminal half of schwannomin and bind to SCHi2 more strongly than SCHi1 as measured by the yeast two-hybrid method. p110 binds the N-terminal domain of SCHi1 or SCHi2 with similar affinity. In the present study we tested the ability for eleven different naturally occurring mutant schwannomins to interact with its binding partners HRSi1, HRSi2, βII-spectrin, and p110, and to self-interact with wild-type (wt-) SCHi1, wt-SCHi2, and N- and C-terminal SCH fragments, using the yeast two-hybrid method. We showed that many of the missense mutations altered the SCH binding properties for HRS, βII-spectrin, and p110, and SCH self-binding.

MATERIALS AND METHODS

Plasmid constructs. The cDNA encoding full-length HRS isoform 1 in vector pGAD10 was obtained by yeast two-hybrid screening and was modified to encode the full-length HRS isoform 2 of 110 kDa as previously described (17). The pGAD10–βII-spectrin construct was obtained by two-hybrid screening and this construct encodes amino acids 1716–1998 of βII-spectrin. The pACT–p110 construct was obtained by two-hybrid screening and this construct encodes amino acids 69–635 of the eIF3 p110 subunit (Scoles and Pulst, in preparation). The pGBT9–Nf2i1 and pGBT9–Nf2i2 plasmids were made as previously described (18). The pGAD10–Nf2i2 construct was made by excising the full-length Nf2i2 from pGBT9–Nf2i2 with *Sma*I and *Bam*HI then ligating in pGAD10 prepared by digesting with *Xho*I, followed by blunt filling with T4 DNA polymerase, then digesting with *Bam*HI. The pGAD10–Nf2i1 construct was made just as was pGAD10–Nf2i2, but starting with pGBT9–SCHi1. The pGBT9–Nf2i1(256–595) construct was made by generating the Nf2i1(256–595) fragment by PCR using primers 5′-GATCGAATTCCCGTGGAATGAAATCCGAAAC-3′ and 5′-TTTGGAATTCTCAAATGCAGATAGGTCTTCT-3′ which was then digested with *Eco*RI and ligated in the *Eco*RI site of pGBT9. The pGBT9-Nf2i2(256–590) construct was made by generating the Nf2i1(256–595) fragment by PCR using primers 5′-GATCGAATTCCCGTGGAATGAAATCCGAAAC-3′ and 5′-GCTGGAATTCCTGCTAGAGCTCTTCAAA-3′ which was then digested with *Eco*RI and ligated in the *Eco*RI site of pGBT9. The pGBT9–Nf2i1(469–595) construct was made by generating the Nf2i1(469–595) fragment by PCR using primers 5′-GCGAGAATTCAAGCAGAAGCTCCTGGAGATT-3′ and 5′-AAGAAACTTCTCGAGATCGTCCTTAAGGTCG-3′ which was then digested with *Eco*RI and ligated in the *Eco*RI site of pGBT9. The pGAD10-Nf2i2(469–590) construct was made by generating the Nf2i2(469–590) fragment by PCR using primers 5′-GCGAGAATTCAAGCAGAAGCTCCTGGAGATT-3′ and 5′-TCTTCTGGATAGAGCTAAACTCTTAAGTTTG-3′ which was then digested with *Eco*RI and ligated in the *Eco*RI site of pGBT9. The pGAD10–Nf2i1(519–595) construct was made by generating the Nf2i1(519–595) fragment by PCR using primers 5′-GCGGGAATTCATGGAGATAGAGAAAGAAAAA-3′ and 5′-AAGAAACTTCTCGAGATCGTCCTTAAGGTCG-3′ which was then digested with *Eco*RI and ligated in the *Eco*RI site of pGBT9. The pGAD10–Nf2i2(519–590) construct was made by generating the Nf2i2(519–590) fragment by PCR using primers 5′- GCGGGAATTCATGGAGATAGAGAAAGAAAAA-3′ and 5′-TCTTCTGGATAGAGCTAAACTCTTAAGTTTG-3′ which was then digested with *Eco*RI and ligated in the *Eco*RI site of pGBT9.

PCR-based site directed mutagenesis. Three PCRs were performed in two steps to produce a fragment of the *Nf2* gene with nucleotide base changes to introduce single amino acid substitution mutations as previously described (18). The mutated PCR products were ligated in place of the normal counterpart excised from pGBT9–Nf2i2.

Two-hybrid tests of interaction. Yeast strain Y190 double-transformants were grown on SC media with leucine, and tryptophane dropped out, and 2% glucose as previously described (18). β-Galactosidase production was assayed using the filter binding assay by incubating freeze-fractured colonies on nitrocellulose in Z-buffer (60 mM Na_2HPO_4, 40 mM NaH_2PO_4, 10 mM KCl, 1 mM $MgSO_4$, pH 7.0, 0.03 mM β-mercaptoethanol, and 2.5 μM X-gal) at 37°C for 15 min to 8 h. We determined the relative strengths of interaction using semiquantitative liquid assays for β-galactosidase by incubating yeast extracted in Z buffer and 5% chloroform with 0.6 mg/ml o-nitrophenyl β-D-galactopyranoside for 40 min. β-Galactosidase units = $1000 \times [OD_{420}/(OD_{600} \times \text{time (in min)} \times \text{culture volume (in ml)})]$ (19).

RESULTS

The locations of the studied *Nf2* missense mutations relative to all known *Nf2* missense mutations are provided in Fig. 1. We tested the ability for wt-SCHi1, wt-SCHi2, and SCHi2 missense mutants to bind HRSi1, HRSi2, βII-spectrin, and p110 using the yeast two-hybrid system (20). The p110 protein interacts with the schwannomin N-terminal half, within schwannomin residues 1–305 (Scoles and Pulst, in preparation). SCHi2 interacted considerably stronger with HRSi1, HRSi2, or βII-spectrin, all of which bind the SCH C-terminal half, than did SCHi1 (Fig. 2). The strength of interaction between SCHi2 and p110 was about equal to that of SCHi1 (Fig. 2). Of the eleven tested schwannomin missense mutations, L46R located in the SCH N-terminal half, decreased interaction with each of the schwannomin binding proteins (Fig. 2). The decrease for HRSi2, βII-spectrin, p110 amounted to a complete loss of interaction, while residual binding remained for HRSi1 (Fig. 2).

Among the tested *Nf2* missense mutations, the effect of those in the C-terminal half of the protein was greatest, resulting in loss or near loss of interaction. Schwannomin with the missense mutation L360P did not interact with HRSi1 or HRSi2, but did interact with βII-spectrin and p110 (Fig. 2). Schwannomin with either of the missense mutations K364I, L535P, or Q538P did not significantly bind to HRSi1, HRSi2, βII-spectrin, or p110 (Fig. 2).

Some *Nf2* missense mutations resulted in elevated schwannomin interaction with HRSi1, HRSi2, βII-spectrin, or p110. These mutations are all located between amino acids 219 and 352. The mutations V219M, N220Y, I273F, and T352M elevated interactions with HRSi1 two- to threefold (Fig. 2). Mutations N220Y and I273F elevated interaction with HRSi2 by 155 and 137%, respectively (Fig. 2). The I273F mutation elevated βII-spectrin binding by 241% (Fig. 2).

To show the effects of schwannomin missense mutations on interactions with other schwannomins, we tested the ability for wt-SCHi1, wt-SCHi2, and SCHi2

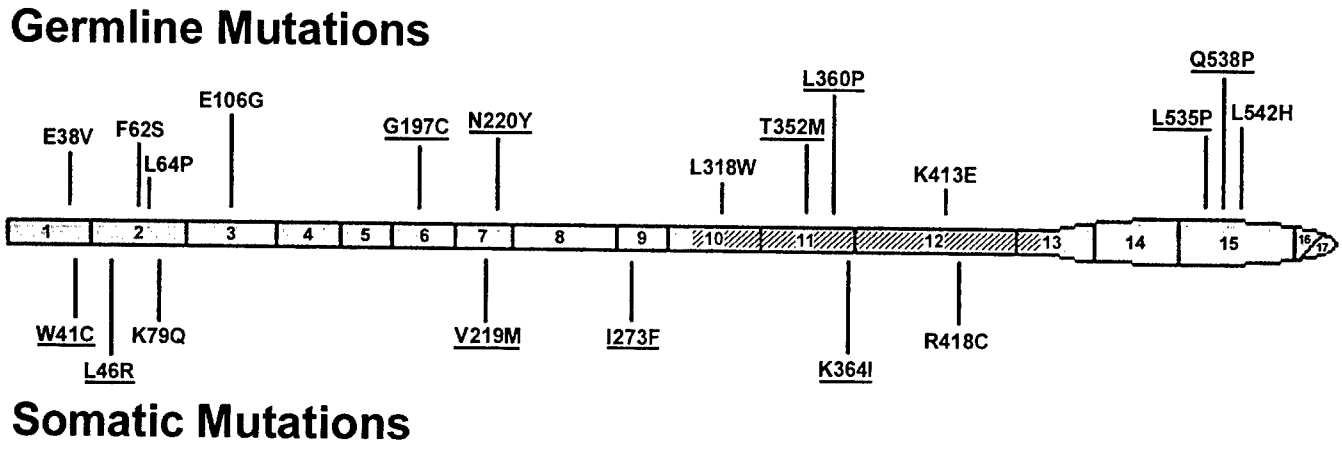

FIG. 1. Schwannomin domains and locations of naturally occurring amino acid substitutions. The N- and C-terminal domains of schwannomin are separated by the α-helical (hatched) central domain. Germline mutations are at the top of the diagram and somatic mutations are at the bottom. Missense mutations that are underlined were included in the study.

missense mutants to bind wt-SCHi1, wt-SCHi2. The interaction of SCHi1 with itself was as strong as with SCHi2, whereas the self-interaction of SCHi2 was stronger that its interaction with SCHi1 (Fig. 3).

Most of the *Nf2* missense mutations had little effect on SCH self-binding, and in general, the mutations decreased SCHi2 binding more than SCHi1 binding. Wt-SCHi1 interaction with wt-SCHi2 was of the approximate same strength as for missense SCHi2 proteins with the W41C, L46R, G197C, V219M, N220Y, I273F, and T352M mutations (Fig. 3). SCHi1 interaction was reduced with SCHi2 proteins mutated at L360P, K364I, L535P, and Q538P (Fig. 3). Most of the tested mutant SCHi2 proteins had decreased interaction with wt-SCHi2 compared to the strength of interaction observed between two wt-SCHi2 proteins (Fig. 3). SCHi2 with the K364I mutation did not bind wt-SCHi2, and SCHi2 with the L46R mutation did not interact with either SCHi1 or SCHi2 (Fig. 3).

We determined that sites for schwannomin self-interaction are different between schwannomin isoform 1 and schwannomin isoform 2 by interacting full-length SCHi1 or SCHi2 with C-terminal fragments of SCHi1 and SCHi2. Strengths of interactions between C-terminal fragments of SCH isoform 1 or isoform 2 (including amino acids 256–595 and 256–590, respectively) and wt-SCHi1 were insignificant (Fig. 4). In contrast, the strengths of interactions between the same C-terminal fragments and full-length SCHi2 was significantly higher than control tests ($P < 0.01$, Student's t test) (Fig. 4).

The masking of binding sites may complicate the interaction between schwannomin and other proteins. To demonstrate this, we determined the strengths of interaction between full-length or C-terminal fragments of SCHi2 or SCHi1 with βII-spectrin using the yeast two-hybrid system. βII-Spectrin interacted more strongly with full-length SCHi2 than SCHi1, and successive N-terminal truncation resulted in loss of βII-spectrin binding (Fig. 5). However, the interaction of SCHi1 C-terminal fragments was stronger than full-length SCHi1, suggesting that the N-terminal half of schwannomin isoform 1 masks a site for βII-spectrin binding in the C-terminal domain (Fig. 5).

The effect of *Nf2* missense mutations on schwannomin interaction with each of the interacting proteins is summarized in Table 1.

DISCUSSION

A general framework for how SCH intramolecular interactions might influence SCH intermolecular interactions can be obtained by comparing SCH to ERM family proteins. The identities between ezrin and schwannomin N-terminal, α-helical, and C-terminal domains are 61, 30, and 22%, respectively (21). Ezrin exists in at least two conformational states, folded monomers and elongated dimers, both containing masked C-terminal domain binding sites for interaction with N-terminal domains of other ERM proteins that are unmasked in both the monomeric and dimeric states (12, 22). Moesin also folds like ezrin in a manner involving interaction between the N- and C-terminal domains (11).

FIG. 2. Yeast two-hybrid tests of interaction between schwannomin isoform 1, schwannomin isoform 2, or schwannomin isoform 2 with the indicated missense mutations and (A) HRSi1 and HRSi2 or (B) βII-spectrin and p110. Each of the SCHi1, SCHi2, or SCHi2 mutant proteins as indicated on the *X*-axis were expressed as fusions to the GAL4 binding domain and tested in yeast cells for interaction with HRSi1, HRSi2, βII-spectrin, or p110 fused to the GAL4 activation domain. Values are β-galactosidase units and are reported as means ± SD of three replicates.

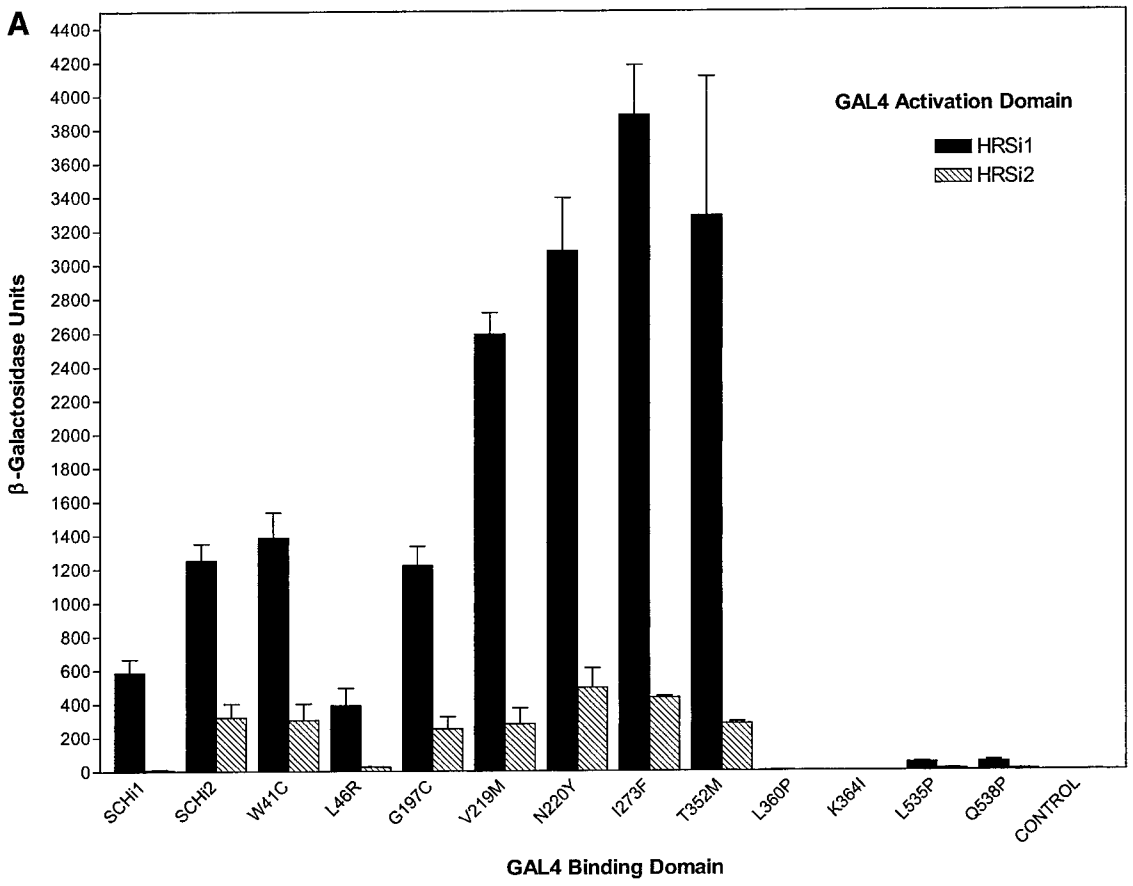
A
β-Galactosidase Units
GAL4 Activation Domain
HRSi1
HRSi2
SCHi1
SCHi2
W41C
L46R
G197C
V219M
N220Y
I273F
T352M
L360P
K364I
L535P
Q538P
CONTROL
GAL4 Binding Domain

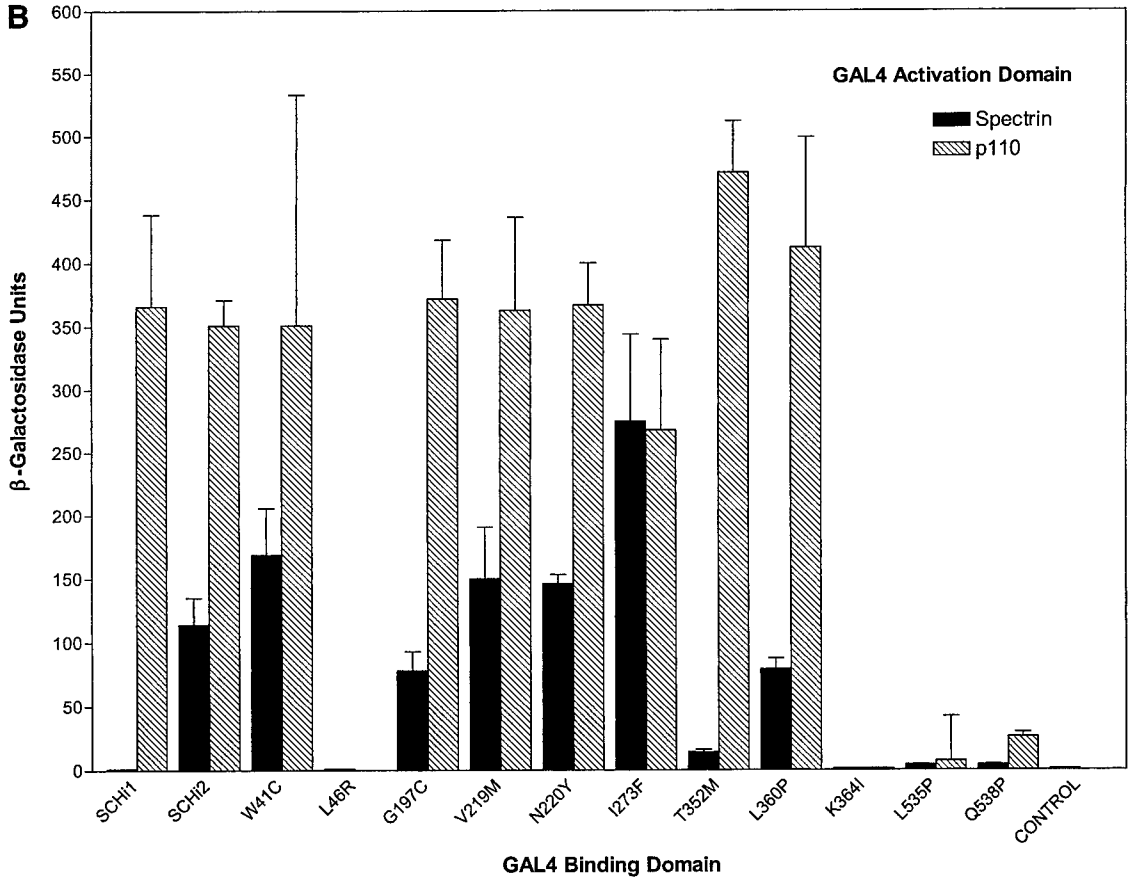
B
β-Galactosidase Units
GAL4 Activation Domain
Spectrin
p110
SCHi1
SCHi2
W41C
L46R
G197C
V219M
N220Y
I273F
T352M
L360P
K364I
L535P
Q538P
CONTROL
GAL4 Binding Domain

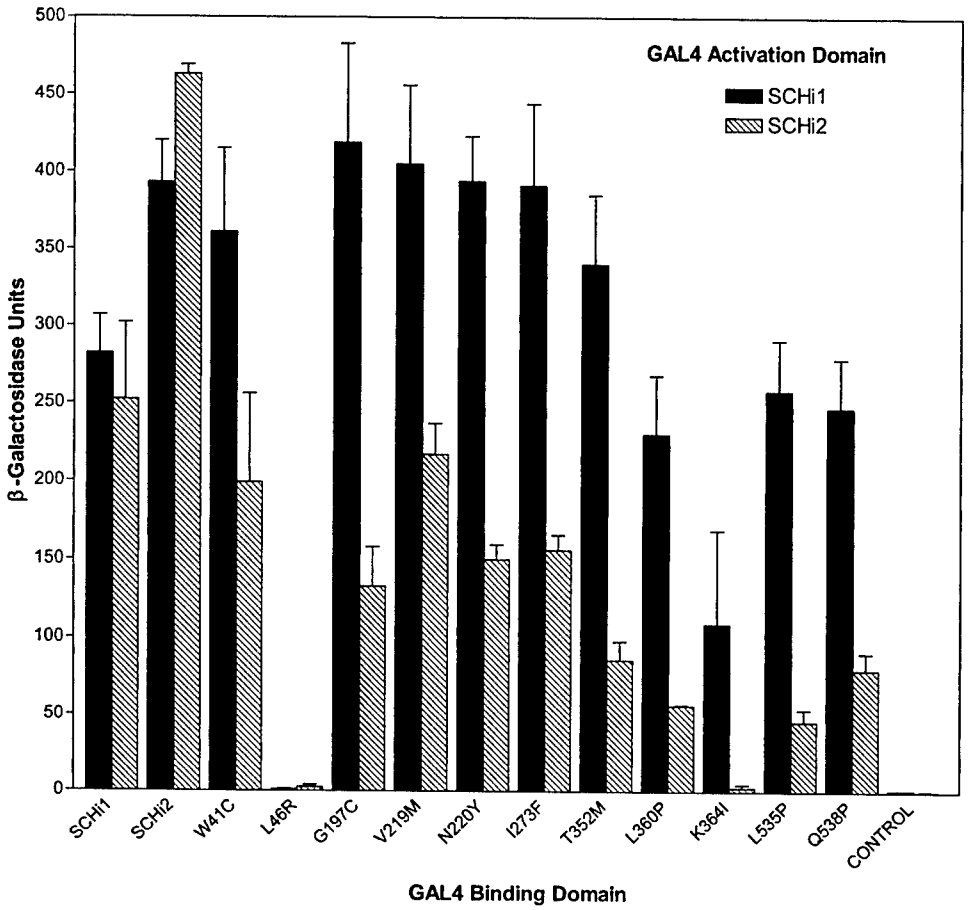

FIG. 3. Yeast two-hybrid tests of interaction between schwannomin isoform 1, schwannomin isoform 2, or schwannomin isoform 2 with the indicated missense mutations and schwannomin isoform 1 or schwannomin isoform 2. Each of the SCHi1, SCHi2, or SCHi2 mutant proteins as indicated on the *X*-axis were expressed as fusions to the GAL4 binding domain and tested in yeast cells for interaction with SCHi1 or SCHi2 fused to the GAL4 activation domain. The control tests show the levels of background obtained in the control interaction between SCHi1 or SCHi2 and the GAL4 binding domain with no fusion. Values are β-galactosidase units and are reported as means ± SD of three replicates.

Schwannomin Folding

Schwannomin folds in a head-to-tail manner. Gutmann *et al.* (23) demonstrated that two intramolecular interactions in schwannomin mediate the folded conformation. One of these occurs between two regions within the schwannomin N-terminal domain (residues 8–121 and 200–320). The other occurs between N-terminal and C-terminal schwannomin regions (residues 302–308 and residues 580–595). The latter N- to C-terminal domain interaction could not be demonstrated in schwannomin isoform 2 (24) or in a L64P schwannomin isoform 1 mutant protein that had lost the ability for N-terminal domain self-association (23). Gutmann *et al.* (23) hypothesized that the N-terminal domain self-association is required for the N- to C-terminal domain interaction to take place. This hypothesis was strongly supported by Grönholm *et al.* (16) who showed that schwannomin N- and C-terminal domain fragments of residues 1–339 and 252–595 interacted, but schwannomin fragments of residues 1–167 and 252–595 did not. But inconsistently, Grönholm *et al.* (16) also showed that a schwannomin fragment of residues 339-585 interacted with schwannomin fragments of residues 1–167 and 252–595. This result suggested that a masked binding site in the C-terminal domain, present in both schwannomin isoforms, interacted with the unfolded N-terminal domain, and placed into question whether schwannomin isoform 2 could undergo folding. This is of particular interest since it is believed that schwannomin must be folded to function as a negative growth regulator (24).

We tested the effects of mutation on schwannomin isoform 2 interactions using the Gal4-based yeast two-hybrid system in the framework of two hypotheses.

Hypothesis I. Any mutation that disrupts schwannomin self-association alters its ability to bind other proteins.

Hypothesis II. Schwannomin isoform 2 is folded differently than schwannomin isoform 1, perhaps explaining why schwannomin isoform 2 is not a negative growth regulator.

TABLE 1

Nf2 Missense Mutation, Mutation Type (Somatic or Germline), Patient Phenotype (for Germline Mutations Only), and Effect on Schwannomin Interaction

Mutation	Somatic/Germline	Patient phenotype	Effect of the mutation on binding
Trp41Cys (25)	Somatic	—	Interacted with all proteins like the nonmutant SCHi2
Leu46Arg (26, 27)	Somatic	—	Disrupted interactions with all proteins, but interacted strongly with HRSi1 and moderately with HRSi2
Gly197Cys (25)	Somatic	—	Interacted with all proteins like the nonmutant SCHi2, but the mutation decreased binding to βII-spectrin and SCHi2
Val219Met (9, 28)	Somatic	—	Interacted with all proteins like the nonmutant SCHi2, but the mutation elevated HRSi1 binding and decreased SCHi2 binding
Asn220Tyr (2)	Germline	Mild	Interacted with all proteins like the nonmutant SCHi2, but the mutation elevated HRSi1 and HRSi2 binding and decreased SCHi2 binding
Ile273Phe (29)	Somatic	—	Interacted with all proteins like the nonmutant SCHi2, but the mutation elevated HRSi1, HRSi2, and βII-spectrin binding and decreased SCHi2 binding
Thr352Met (30)	Germline	Severe	Interacted with all proteins like the nonmutant SCHi2, but the mutation elevated HRSi1 and βII-spectrin binding and decreased SCHi2 binding
Leu360Pro (7, 26)	Germline	Mild	The mutation did not alter p110 binding, but disrupted interaction with HRSi1 and HRSi2 and weakened binding to βII-spectrin, SCHi1, and SCHi2
Lys364Ile (29)	Somatic	—	The mutation weakened binding to SCHi1 and disrupted binding to HRSi1, HRSi2, βII-spectrin, p110, and SCHi2
Leu535Pro (31)	Germline	Mild	The mutation weakened interaction with HRSi1, HRSi2, βII-spectrin, p110, and SCHi2
Gln538Pro (32)	Germline	Mild/Severe	The mutation weakened interaction with HRSi1, HRSi2, βII-spectrin, p110, and SCHi2

Our approach to test hypothesis I was to assess the ability for full-length schwannomin isoform 1, isoform 2, and isoform 2 mutants (Fig. 1) to interact with HRSi1, HRSi2, βII-spectrin, p110 and with wild-type schwannomin isoform 1 and isoform 2. The second hypothesis was tested by comparing the binding of C-terminal fragments with that of full-length proteins.

In some cases, interactions in yeast may not wholly reflect interactions in mammalian cells. For example, Meng *et al.* (33) showed SCHi1 and ezrin interacted by coimmunoprecipitation of overexpressed proteins from A431 cells, but the authors were unable to show these two proteins interacted using a transcriptionally based yeast two-hybrid method. In the Gal4-based yeast two-hybrid method, the SCHi1-ezrin protein complex may fail to translocate to the nucleus, or perhaps the conformation of the complex does not allow the Gal4 activation domain the correct positioning for transcriptional activation. In addition, while yeast two-hybrid experiments cannot address the stability of missense or nonsense containing transcripts under physiologic conditions, they can make important contributions to structure/function studies. However, comparisons of the β-galactosidase values among Figs. 2 and 3 suggest that all mutant constructs were similarly expressed in yeast.

Effect of Nf2 Mutation on Binding to HRS, βII-Spectrin, and p110

Nf2 mutations significantly altered schwannomin binding to HRS, βII-spectrin, and p110. Schwannomin isoform 2 mutated at L46R had reduced or no binding to HRS isoform 2 and βII-spectrin, which interact with the schwannomin C-terminal half, and p110 which binds the schwannomin N-terminal half (Fig. 2). L46 is within the region involved in N-terminal domain folding (23). Schwannomin binding to each of HRS, βII-spectrin, or p110 was abolished by mutations K364I, L535P, and Q538P. The crystal structure of moesin showed that the surface residues where contact is made between the N- and C-terminal domains share 81% identity to schwannomin, suggesting a similar mechanism in schwannomin folding (11). Because moesin residues V518 and H521, which lie on the interface where the moesin N- and C-terminal domains make contact, correspond to schwannomin residues L535 and Q538 (11), schwannomin mutations at these locations are likely to alter schwannomin folding and binding properties. Missense mutations in the middle domain of SCH (V219M, N220Y, I273F, and T352M) elevated strengths of interactions with HRS and βII-spectrin. The elevated interaction may be of no consequence to SCH loss of function, or may result in loss of schwannomin-mediated signaling due to irreversible binding. Schwannomin isoform 2 mutated at L46R, K364I, L535P, or Q538P is either misfolded or in an otherwise unfavorable conformation that denies sites for binding.

Effect of Nf2 Mutation on Binding of Other SCH Proteins

Only two *Nf2* mutations abolished schwannomin isoform 2 binding to other schwannomin proteins as well

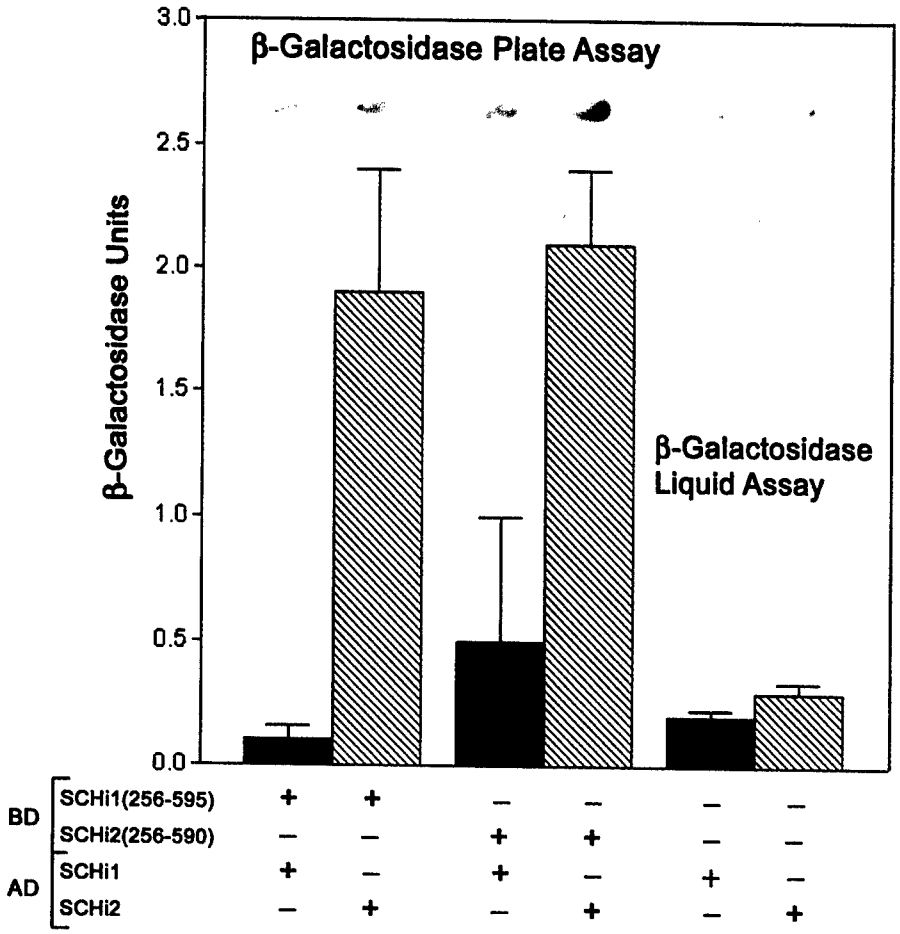

FIG. 4. Yeast two-hybrid tests of interaction between schwannomin isoform 1 or 2 and schwannomin isoform 1 or 2 C-terminal fragments. SCHi1(256–595) and SCHi2(256–590) were expressed as fusions to the GAL4 binding domain (BD) and tested in yeast cells for interaction with SCHi1 or SCHi2 fused to the GAL4 activation domain (AD). The control tests show the levels of background obtained in the control interaction between SCHi1 or SCHi2 and the GAL4 binding domain with no fusion. For the plate assay data, blue indicates the presence of β-galactosidase and a positive interaction. For the liquid assay values given are β-galactosidase units, reported as means ± SD of three replicates.

as to other schwannomin interacting proteins. The schwannomin isoform 2 mutated at L46R failed to interact with either wild-type SCHi1 or SCHi2, demonstrating that this mutant does not self-associate (Fig. 3). Schwannomin isoform 1 and 2 differed remarkably in their affinity for binding SCHi2 mutated at K364I. Schwannomin isoform 1 interacted with the K364I mutant while SCHi2 did not (Fig. 3). The SCHi2 mutated at K364I also had reduced affinity for SCHi1 compared to all other mutant SCHi2 proteins except L46R (Fig. 3). HRS, βII-spectrin or p110 did not interact with SCHi2 mutated at K364I. Our hypothesis I is strongly upheld for L46R and K364I. In addition, the mutations L535P, and Q538P that reduced but did not abolish schwannomin self-interaction had significant effect on schwannomin interaction with HRS, βII-spectrin and p110. Likewise, the mutation L360P that reduced but did not abolish schwannomin self-interaction had significant effect on schwannomin interaction with HRS, but did not disrupt schwannomin binding with βII-spectrin or p110.

Full-Length SCH Isoform 2 Can Bind SCH C-Terminal Domain of Either Isoform

We tested the hypothesis II that schwannomin isoform 2 is unable to fold like schwannomin isoform 1 by assessing the ability for SCHi1 or SCHi2 C-terminal domain fragments (residues 256–595 and 256–590, respectively) to bind full-length SCHi1 or SCHi2. Full-length schwannomin isoform 1 did not interact with the C-terminal fragment of either isoform while full-length schwannomin isoform 2 interacted with the C-terminal fragments of both isoforms (Fig. 4). The schwannomin isoform 1 may be so strongly folded in our assay that a binding site for the C-terminal fragment of schwannomin isoform 1 was masked. Schwannomin isoform 2, which previously was believed to not

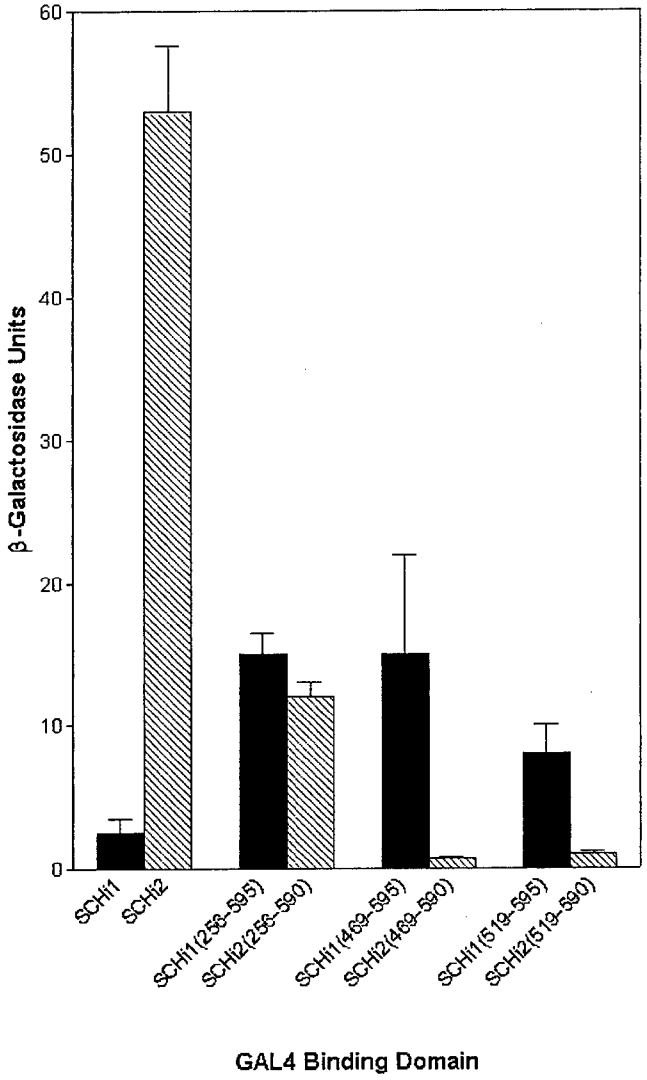

FIG. 5. Yeast two-hybrid tests of interaction between βII-spectrin and full-length or truncated schwannomin isoform 1 (black) or schwannomin isoform 2 (hatched) proteins. Each of the schwannomin proteins indicated on the *X*-axis were expressed as fusions to the GAL4 binding domain and tested in yeast cells for interaction with βII-spectrin residues 1716–1998 fused to the GAL4 activation domain. The control tests show the levels of background obtained in the control interaction between SCHi1 or SCHi2 and the GAL4 binding domain with no fusion. Values are β-galactosidase units and are reported as means ± SD of three replicates.

undergo N- to C-terminal domain folding, interacted with the C-terminal fragments of both isoforms. Thus we conclude that a site that binds the C-terminal half of either isoform of schwannomin is available in the full-length schwannomin isoform 2 that is unavailable in schwannomin isoform 1 in our assay. This is likely due to differences in the folding strengths of the full-length proteins. Schwannomin isoform 2 may undergo N- to C-terminal domain folding in a manner that is entirely different from that in schwannomin isoform 1.

Schwannomin Isoforms Bind βII-Spectrin Uniquely

Because the interactions between schwannomin C-terminal fragments and full-length proteins were all exceedingly weak (Fig. 4), we supported the conclusions of those tests, that schwannomin isoforms 1 and 2 fold uniquely, by testing the ability for truncated schwannomin proteins to bind βII-spectrin. Interactions by SCHi1 and SCHi2 for βII-spectrin and SCHi2 L46R support that the schwannomin isoforms are differently folded and present some unique binding properties. We previously showed that C-terminal fragments of schwannomin interacted with βII-spectrin (18). We have now compared βII-spectrin binding affinities between the schwannomin isoforms using matched sets of C-terminal domain fragments in effort to identify differences in schwannomin isoform conformations. We found that deletion of residues 1–255 markedly decreased SCHi2 affinity for βII-spectrin, but allowed SCHi1 to more strongly bind βII-spectrin (Fig. 5). Further truncation abolished βII-spectrin binding by SCHi2, but not by SCHi1 (Fig. 5). βII-Spectrin binding properties are remarkably unique between the two schwannomin isoforms. The βII-spectrin binding site is masked in full-length schwannomin isoform 1 but not 2, and in truncated schwannomin isoform 2 but not 1.

Our hypothesis II is strongly supported by these tests. The data strongly show that the schwannomin isoform 2 folded conformation is unique from that of schwannomin isoform 1. We further hypothesize that the differences in growth regulatory properties between schwannomin isoform 1 and 2 result from differences in protein binding or folded conformations.

Mutation in the *Nf2* gene severely affects schwannomin normal function by disrupting interactions between schwannomin with itself and its interacting proteins. Schwannomin isoform 1 is a verified growth suppressor while no such function has been proven for schwannomin isoform 2 (24). The growth suppressor function in schwannomin isoform 1 has been tied to schwannomin intramolecular interactions (23). We now show that unique inter- and intramolecular interactions occur for schwannomin isoform 2, suggesting that this schwannomin isoform has unique functional properties.

ACKNOWLEDGMENTS

This work was supported by the Carmen and Louis Warschaw Endowment Fund, Grant NS01428-01A1 from the National Institutes of Health, and Grant DAMD17-99-1-9548 from the Department of Defense to S.-M.P. and by NIH National Research Service Award NS10524-02 to D.R.S. Paul Morcos assisted with site-directed mutagenesis.

REFERENCES

1. Sainz, J., Huynh, D. P., Figueroa, K., Ragge, N. K., Baser, M. E., and Pulst, S. M. (1994) Mutations of the neurofibromatosis type 2 gene and lack of the gene product in vestibular schwannomas. *Hum. Mol. Genet.* **3,** 885–891.

2. Ruttledge, M. H., Andermann, A. A., Phelan, C. M., Claudio, J. O., Han, F. Y., Chretien, N., Rangaratnam, S., MacCollin, M., Short, P., Parry, D., Michels, V., Riccardi, V. M, Weksberg, R., Kitamura, K., Bradburn, J. M., Hall, B. D., Propping, P., and Rouleau, G. A. (1996) Type of mutation in the neurofibromatosis 2 gene (NF2) frequently determines severity of disease. *Am. J. Hum. Genet.* **59,** 331–342.
3. Rubio, M. P., Correa, K. M., Ramesh, V., MacCollin, M. M., Jacoby, L. B., von Deimling, A., Gusella, J. F., and Louis, D. N. (1994) Analysis of the neurofibromatosis 2 gene in human ependymomas and astrocytomas. *Cancer Res.* **54,** 45–47.
4. Gutmann, D. H., Giordano, M. H., Fishback, A. S., and Guha, A. (1997) Loss of merlin expression in sporadic meningiomas, ependymomas and schwannomas. *Neurology* **49,** 267–270.
5. Huynh, D. P., Mautner, V., Baser, M. E., Stavrou, D., and Pulst, S. M. (1997) Immunohistochemical detection of schwannomin and neurofibromin in vestibular schwannomas, ependymomas and meningiomas. *J. Neuropathol. Exp. Neurol.* **56,** 382–390.
6. Mautner, V. F., Lindenau, M., Baser, M. E., Hazim, W., Tatagiba, M., Hasse, W., Samii, M., Wais, R., and Pulst, S. M. (1996) The neuroimaging and clinical spectrum of neurofibromatosis 2. *Neurosurgery* **38,** 880–885.
7. Rouleau, G. A., Merel, P., Lutchman, M., Sanson, M., Zucman, J., Marineau, C., Xuan, K. H., Demczuk, S., Desmaze, C., Plougastel, B., Pulst, S.-M., Lenoir, G., Bijlsma, E., *et al.* (1993) Alteration in a new gene coding a putative membrane-organizing protein causes neuro-fibromatosis type 2. *Nature* **363,** 515–521.
8. Trofatter, J. A., MacCollin, M. M., Rutter, J. L., Murrell, J. R., Duyao, M. P., Parry, D. M., Eldridge, R., Kley, N., Menon, A., Pulaski, K., Haase, V. H., Ambrose, C. M., Munroe, D., *et al.* (1993) A novel moesin-, ezrin-, radixin-like gene is a candidate for the neurofibromatosis 2 tumor suppresser. *Cell* **72,** 791–800.
9. Jacoby, L. B., MacCollin, M., Louis, D. N., Mohney, T., Rubio, M. P., Pulaski, K., Trofatter, J. A., Kley, N., Seizinger, B., Ramesh, V., *et al.* (1994) Exon scanning for mutation of the NF2 gene in schwannomas. *Hum. Mol. Genet.* **3,** 413–419.
10. Huynh, D. P., Nechiporuk, T., and Pulst, S.-M. (1994) Alternative transcripts in the mouse neurofibromatosis type 2 (NF2) gene are conserved and code for schwannomins with distinct C-terminal domains. *Hum. Mol. Genet.* **3,** 1075–1079.
11. Pearson, M. A., Reczek, D., Bretscher, A., and Karplus, P. A. (2000) Structure of the ERM protein moesin reveals the FERM domain fold masked by an extended actin binding tail domain. *Cell* **101,** 259–270.
12. Gary, R., and Bretscher, A. (1995) Ezrin self-association involves binding of an N-terminal domain to a normally masked C-terminal domain that includes the F-actin binding site. *Mol. Biol. Cell* **6,** 1061–1075.
13. Reczek, D., Berryman, M., and Bretscher, A. (1997) Identification of EBP50: A PDZ-containing phosphoprotein that associates with members of the ezrin–radixin–moesin family. *J. Cell Biol.* **139,** 169–179.
14. Bretscher, A, Gary, R., and Berryman, M. (1995) Soluble ezrin purified from placenta exists as stable monomers and elongated dimers with masked C-terminal ezrin–radixin–moesin association domains. *Biochemistry* **34,** 16830–16837.
15. Xu, H. M., and Gutmann, D. H. (1998) Merlin differentially associates with the microtubule and actin cytoskeleton. *J. Neurosci. Res.* **51,** 403–415.
16. Grönholm, M., Sainio, M., Zhao, F., Heiska, L., Vaheri, A, and Carpen, O. (1999) Homotypic and heterotypic interaction of the neurofibromatosis 2 tumor suppressor protein merlin and the ERM protein ezrin. *J. Cell Sci.* **112**(Pt. 6), 895–904.
17. Scoles, D. R., Huynh, D. P., Chen, M. S., Burke, S. P., Gutmann, D. H., and Pulst, S. M. (2000) The neurofibromatosis 2 (NF2) tumor suppressor protein interacts with hepatocyte growth factor-regulated tyrosine kinase substrate, HRS. *Hum. Mol. Genet.* **9,** 1567–1574.
18. Scoles, D. R., Huynh, D. P., Coulsell, E. R., Robinson, N. G. G., Tamanoi, F., and Pulst, S.-M. (1998) The neurofibromatosis 2 tumor suppressor schwannomin interacts with βII-spectrin (fodrin). *Nat. Genet.* **18,** 354–359.
19. Poullet, P., and Tamanoi, T. (1995) Use of yeast two-hybrid system to evaluate ras interactions with neurofibromin GTPase-activating proteins. *Methods Enzymol.* **255,** 488–497.
20. Fields, S., and Song, O.-k. (1989) A novel genetic system to detect protein–protein interactions. *Nature* **340,** 245–246.
21. Turunen, O., Sainio, M., Jaaskelainen, J., Carpen, O., and Vaheri, A. (1998) Structure–function relationships in the ezrin family and the effect of tumor-associated point mutations in neurofibromatosis 2 protein. *Biochim. Biophys. Acta* **1387,** 1–16.
22. Bretscher, A., Reczek, D., and Berryman, M. (1997) Ezrin: A protein requiring conformational activation to link microfilaments to the plasma membrane in the assembly of cell surface structures. *J. Cell Sci.* **110**(Pt. 24), 3011–3018.
23. Gutmann, D. H., Haipek, C. A., and Lu, K. H. (1999) Neurofibromatosis 2 tumor suppressor protein, merlin, forms two functionally important intramolecular associations. *J. Neurosci. Res.* **58,** 706–716.
24. Sherman, L., Xu, H. M., Geist, R. T., Saporito-Irwin, S., Howells, N., Ponta, H., Herrlich, P., and Gutmann, D. (1997) Interdomain binding mediates tumor growth suppression by the *NF2* gene product. *Oncogene* **15,** 2505–2509.
25. Welling, D. B., Guida, M., Goll, F., Pearl, D. K., Glasscock, M. E., Pappas, D. G., Linthicum, F. H., Rogers, D., and Prior, T. W. (1996) Mutational spectrum in the neurofibromatosis type 2 gene in sporadic and familial schwannomas. *Hum. Genet.* **98,** 189–193.
26. Merel, P., Haong-Kuan, K., Sanson, M., Moreau-Aubry, A., Bijlsma, E. K., Lazaro, C., Moisan, J. P., Resche, F., Nishisho, I., Estivill, X., *et al.* (1995) Predominant occurrence of somatic mutations of the NF2 gene in meningiomas and schwannomas. *Genes Chrom. Cancer* **13,** 211–216.
27. Irving, R., Moffat, D. A., Hardy, D. G., Barton, D. E., Xuereb, J. H., and Maher, E. R. (1994) Somatic NF2 gene mutations in familial and non-familial vestibular schwannoma. *Hum. Mol. Genet.* **3,** 347–350.
28. Merel, P., Khe, H. X., Sanson, M., Bijlsma, E., Rouleau, G., Laurent-Puig, P., Pulst, S., Baser, M., Lenoir, G., Sterkers, J. M., *et al.* (1995) Screening for germ-line mutations in the *NF2* gene. *Genes Chrom. Cancer* **12,** 117–127.
29. Bianchi, A. B., Hara, T., Ramesh, V., Gao, J., Klein-Szanto, A. J., Morin, F., Menon, A. G., Trofatter, J. A., Gusella, J. F., Seizinger, B. R., *et al.* (1994) Mutations in transcript isoforms of the neurofibromatosis 2 gene in multiple human tumour types. *Nat. Genet.* **6,** 185–192.
30. Bourn, D., Carter, S. A., Evans, D. G. R., Goodship, J., Coakham, H., and Strachan, T. (1994) A mutation in the neurofibromatosis type 2 tumor-suppressor gene, giving rise to widely different clinical phenotypes in two unrelated individuals. *Am. J. Hum. Genet.* **55,** 69–73.
31. Bourn, D., Evans, G., Mason, S., Tekes, S., Trueman, L., and Strachan, T. (1995) Eleven novel mutations in the NF2 tumour suppressor gene. *Hum. Genet.* **95,** 572–574.
32. Kluwe, L., and Mautner, V. F. (1996) A missense mutation in the NF2 gene results in moderate and mild clinical phenotypes of neurofibromatosis 2. *Hum. Genet.* **97,** 224–227.
33. Meng, J. J., Lowrie, D. J., Sun, H., Dorsey, E., Pelton, P. D., Bashour, A. M., Groden, J., Ratner, N., and Ip, W. (2000) Interaction between two isoforms of the NF2 tumor suppressor protein, merlin, and between merlin and ezrin, suggests modulation of ERM proteins by merlin. *J. Neurosci. Res.* **62,** 491–502.

Human Molecular Genetics, 2002, Vol. 11, No. 25 3179–3189

Neurofibromatosis 2 (NF2) tumor suppressor schwannomin and its interacting protein HRS regulate STAT signaling

Daniel R. Scoles[1,*], Vu D. Nguyen[1], Yun Qin[1], Chun-Xiao Sun[2], Helen Morrison[3], David H. Gutmann[2] and Stefan-M. Pulst[1,4]

[1]Neurogenetics Laboratory, CSMC Burns and Allen Research Institute, Cedars-Sinai Medical Center, School of Medicine, University of California at Los Angeles, 8700 Beverly Boulevard, Los Angeles, CA 90048, USA, [2]Department of Neurology, Washington University of Medicine, St Louis, MO 63110, USA, [3]Forschungszentrum Karlsruhe, Institut fur Genetik, Karlsruhe, Germany and [4]Division of Neurology, Cedars-Sinai Medical Center, University of California at Los Angeles School of Medicine, Los Angeles, CA 90048, USA

Received August 10, 2002; Revised and Accepted October 4, 2002

Mutations in the neurofibromatosis 2 (*NF2*) gene with the resultant loss of expression of the NF2 tumor suppressor schwannomin are one of the most common causes of benign human brain tumors, including schwannomas and meningiomas. Previously we demonstrated that the hepatocyte growth factor-regulated tyrosine kinase substrate (HRS) strongly interacts with schwannomin. HRS is a powerful regulator of receptor tyrosine kinase trafficking to the degradation pathway and HRS also binds STAM. Both of these actions for HRS potentially inhibit STAT activation. Therefore, we hypothesized that schwannomin inhibits STAT activation through interaction with HRS. We now show that both schwannomin and HRS inhibit Stat3 activation and that schwannomin suppresses Stat3 activation mediated by IGF-I treatment in the human schwannoma cell line STS26T. We also find that schwannomin inhibits Stat3 and Stat5 phosphorylation in the rat schwannoma cell line RT4. Schwannomin with the pathogenic missense mutation Q538P fails to bind HRS and does not inhibit Stat5 phosphorylation. These data are consistent with the hypothesis that schwannomin requires HRS interaction to be fully functionally active and to inhibit STAT activation.

INTRODUCTION

Neurofibromatosis 2 (NF2) is an autosomal dominant disorder caused by mutations in the *NF2* gene. The inherited disorder is characterized by bilateral vestibular schwannomas and a predisposition to multiple benign tumors of the brain and peripheral nervous system. The tumors seen in NF2 patients occur more frequently as sporadic tumors as a consequence of somatic *NF2* mutation. Virtually all sporadic schwannomas bear *NF2* mutations or deletions and *NF2* gene alterations are also common in meningiomas and ependymomas (1–4).

The *NF2* gene encodes the tumor suppressor protein schwannomin or merlin, which has homology to members of the protein 4.1/ERM family of proteins that link the plasma membrane to the cytoskeleton (5,6). Schwannomin closely resembles the ERM proteins ezrin, radixin and moesin, which interact with themselves and with other ERM proteins (7). Since the identification of the *NF2* gene, significant advances have been made in determining schwannomin function. Schwannomin is a multifunctional protein that binds or complexes with a variety of other proteins, including syntenin (8), SCHIP1 (9), CD44 (10), EBP50/NHERF (11,12), Rho GDP dissociation inhibitor (13), other ERM proteins (14–16), βII-spectrin (17), Paxillin (18) and both polymerized actin and microtubules (19). The multitude of interactions suggest that schwannomin probably participates in a variety of signaling pathways mediated by the plasma membrane and cytoskeleton.

Despite the many known interactions for schwannomin, pathways by which schwannomin suppresses tumor growth remain undefined. Schwannomin may have a role in maintaining normal signaling mediated by the actin cytoskeleton as abnormal stress fiber structure results upon schwannomin loss (20–22). In addition, overexpression of schwannomin results in impairment of cell spreading, attachment and motility, which are mediated by the actin cytoskeleton (23). Schwannomin appears to act in the signaling pathways mediated by the small GTP binding proteins Rho and Rac in human fibroblasts, which

*To whom correspondence should be addressed. Tel: +1 3104237374; Fax: +1 3104230149; Email: scolesd@cshs.org

regulate lamellipodial outgrowth (20). More recently schwannomin was shown to be phosphorylated by p21-activated kinase 2 (PAK2) in response to signals mediated by Rac/Cdc42 (24–26).

We identified hepatocyte growth factor-regulated tyrosine kinase substrate (HRS) as a protein binding to the NF2 tumor suppressor schwannomin (27). Tests of the interaction strengths using a yeast two-hybrid-based assay showed that the interaction between the two proteins was exceptionally strong compared with other schwannomin interacting proteins (27,28). HRS is a FYVE-domain protein that binds endosome-associated phosphatidylinositol (3) phosphate [PtdIns(3)*P*] and possesses a ubiquitin interacting motif (UIM) (29–31). HRS is a powerful regulator of trafficking of ubiquitinated receptor tyrosine kinases (RTKs) to the lysosome (31–33). We previously co-localized schwannomin and HRS to EEA1 positive early endosomes, suggesting that schwannomin might have a role in HRS-mediated receptor trafficking (27). HRS also interacts with and inhibits the signal transducing activator molecule STAM, an activator of Janus kinases and inhibits DNA synthesis in BAF-B03 cells (34,35). We also demonstrated that schwannomin and HRS similarly function to inhibit proliferation of RT4 cells (15). Because HRS probably facilitates the degradation of receptors in the lysosome and inhibits STAM, we hypothesized that schwannomin and HRS can inhibit one common output of both of these events: activation of signal transducers and activators of transcription (STATs). We now show that both schwannomin and HRS are inhibitors of STAT activation in human and mouse schwannoma cell lines. Schwannomin with a naturally occurring *NF2* missense mutation that alters HRS binding abolishes the ability for schwannomin to inhibit STAT activation.

RESULTS

Schwannomin and HRS reduce STAT activity

We measured the effect of HRS and schwannomin overexpression on STAT activity using a STAT-responsive luciferase reporter construct pLucTKSIE containing the *sis* inducible element (SIE) upstream of the TK (thymidine kinase) minimal promoter element. Each assay was controlled with a paired assay using pLucTK, containing only the TK minimal promoter element. The utility of these reporter constructs for the study of STAT activation has been previously validated (36). Each of HRSi1, SCHi1 and SCHi2 inhibited SIE activation in a dosage-dependent manner in STS26T cells (Fig. 1A–C). Under the conditions of our model system, 9 μg of schwannomin isoform 2 reduced SIE activity by 84% compared with the vector control, while Q538 schwannomin isoform II reduced SIE activity by only 42%. However, 3 μg of schwannomin isoform II reduced SIE activity by 30%, in contrast to 3 μg of Q538 schwannomin isoform II, which reduced SIE activity by only 4%. Therefore, in our model system, the Q538P mutation reduces the ability of schwannomin to inhibit SIE activation by 50–88% (Fig. 1B).

We also determined the ability of SCHi2 to inhibit SIE activation in RT4 cells. Schwannomin isoform II inhibited SIE to about the level of the TK control in these cells (Fig. 1D). Because SIE is activated by more than one type of STAT protein, we used an additional construct that specifically detects Stat3 activation via the Stat3 inducible element S3 (36). We showed that both SCHi2 and HRSi1 suppressed the S3 element in a dosage-dependent manner (Fig. 1E). In all experiments, transfection of plasmids encoding SCHi1, SCHi2, HRSi1 and Q538P SCHi2 resulted in strong protein expression in STS26T cells (Fig. 1F).

Overexpression of schwannomin alters Stat3 nuclear translocation

To determine the effect of schwannomin on Stat3 subcellular localization, we overexpressed schwannomin in STS26T cells. We determined the degree of Stat3 nuclear translocation in response to overexpression of schwannomin by counting STS26T cell nuclei labeling with Stat3 antibody after transient transfection of Xpress-epitope tagged schwannomin isoform II (SCHi2). We photographed 107 cells including 23 transfected with Xpress-SCHi2. Nuclear Stat3 labeling was scored with the investigator blinded to the transfection status (0 = not different than cytoplasmic labeling, to 4 = intense nuclear labeling). The average scores were highly significantly different between transfected and untransfected cells (0.70 ± 0.76 for transfected cells, 2.38 ± 0.71 for untransfected cells, Student's t probability <0.001), showing that schwannomin significantly inhibited Stat3 nuclear translocation. Examples are shown in Figure 2A–F. Transfection with GFP did not result in changes of nuclear STAT (data not shown).

To support the data obtained by transient overexpression, we employed an inducible (Tet-on) RT4-*NF2* cell line that overexpressed schwannomin isoform I upon treatment with doxycycline (15). As demonstrated above, induction of schwannomin resulted in reduced nuclear Stat3 labeling compared with uninduced cells by confocal microscopy (Fig. 2G–J).

IGF-I stimulates proliferation of RT4 cells

Previous studies have demonstrated that IGF-I is a Schwann cell mitogen (37,38). In 293T cells and other cell types, IGF-I also stimulates the activation of Stat3 (39). To determine the effect of IGF-I on RT4 cell proliferation, we measured thymidine incorporation after IGF-I treatment and demonstrated increased proliferation in response to 100 ng/ml IGF-I. The increased RT4 cell proliferation was equivalent to that observed with HGF, another potent Schwann cell mitogen (40). Upon induction of schwannomin with doxycycline, we observed a reduction in IGF-1 induced cell proliferation (Fig. 3). These data support the hypothesis that schwannomin inhibits cell proliferation in a STAT-dependent fashion.

Schwannomin inhibits IGF-I-mediated Stat3 activation

Based on the results demonstrating that schwannomin inhibits IGF-I-mediated cell proliferation and Stat3 subcellular localization, we next assessed the ability of schwannomin isoform I to inhibit Stat3 phosphorylation in RT4 and STS26T cells. A decreased abundance of phosphorylated Stat3 relative to total

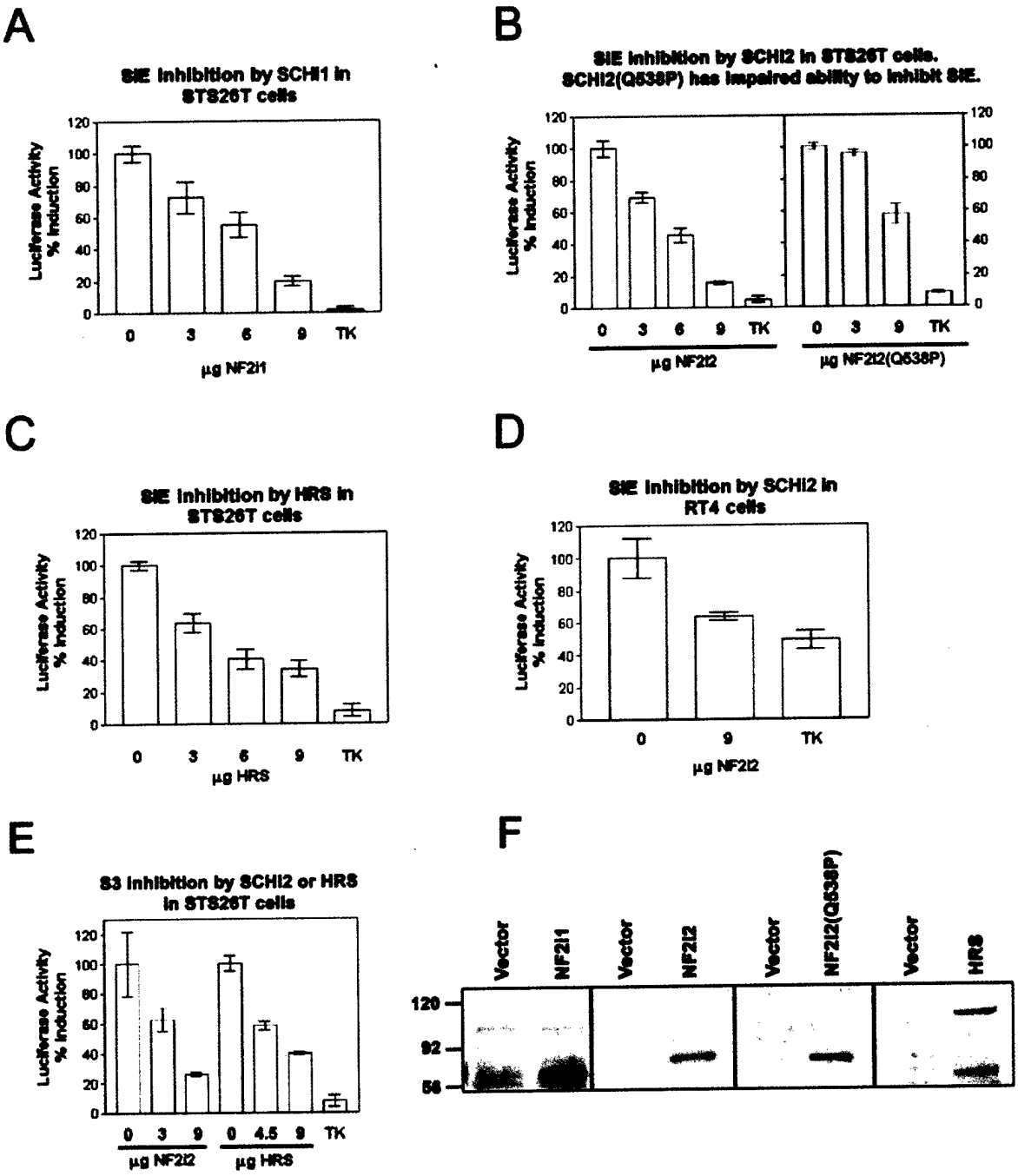

Figure 1. Effects of HRS and schwannomin on inhibition of STAT activation in STS26T and RT4 cells. STS26T cells were transfected with pLukTK or pLukTKSIE and increasing amounts of plasmids that express (**A**) schwannomin isoform I, (**B**) schwannomin isoform II or Q538P schwannomin isoform II, or (**C**) HRS. (**D**) RT4 cells were transfected with pLukTK or pLukTKSIE and increasing amounts of plasmid expressing schwannomin isoform II. (**E**) STS26T cells were transfected with pLukTK or pLukTKS3 and increasing amounts of plasmids that express schwannomin isoform II or HRS. Cells were transiently transfected and luciferase reporter activities were measured as light emission with a luminometer. The results shown are mean ± standard deviation of triplicate measures. (**F**) Immunoblot analysis of expressed proteins. The expression plasmids for schwannomin isoform I and II, HRS and Q538P schwannomin isoform II express proteins with an N-terminal Xpress epitope tag. Proteins of the predicted sizes were detected using the anti-Xpress antibody. Note that Xpress-tagged schwannomin isoform II migrates slower than isoform I with the identical tag. This holds for the GFP tag as well. Proteins expressed by *NF2* cDNAs from these very same constructs without N-terminal tags show an identical electrophoretic migration pattern.

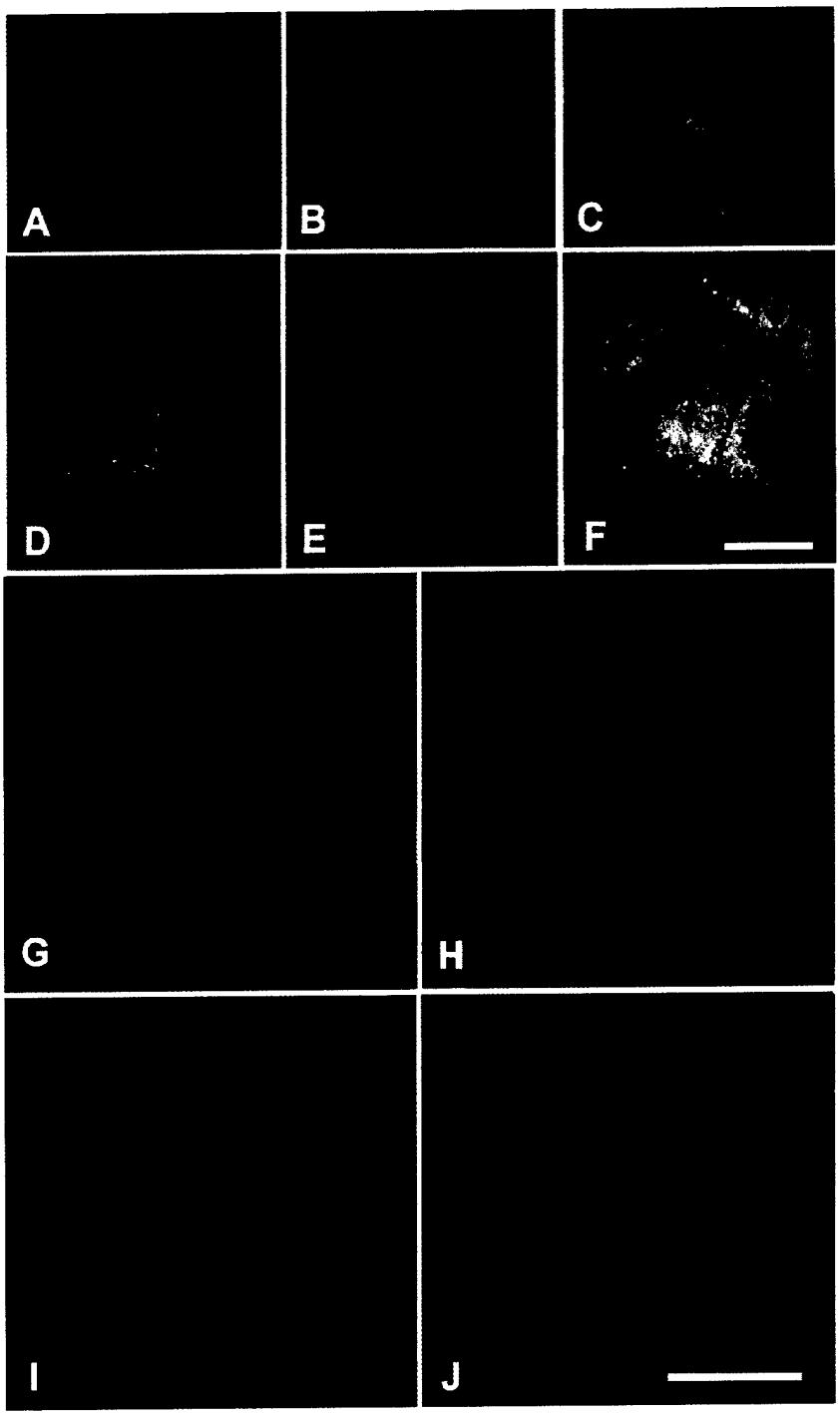

Figure 2. Overexpression of schwannomin alters Stat3 subcellular localization. (**A–F**): STS26T cells were transfected with Xpress-epitope tagged schwannomin isoform II, and co-labeled with anti-Xpress and anti-Stat3 antibodies. A transfected cell labeled with anti-Xpress antibody (A) had very little nuclear Stat3 compared with non-transfected cells, demonstrated by labeling the same cells with anti-Stat3 antibody and immunofluorescent confocal microscopy (B). Overlay of A and B (C). Another example of a transfected STS26T cell labeled with anti-Xpress antibody (D) with little nuclear Stat3 compared to non-transfected cells (E). Overlay of D and E (**F**). (**G–J**) Stat3 observed in Tet-on RT4 NF2.17 without doxycycline, detected by immunofluorescent confocal microscopy, was more strongly nuclear (G and H) than in these cells grown at the same time and under identical conditions but with doxycycline (I and J). These cells were photographed with equal exposures and digital contrast. Bar = 40 μm.

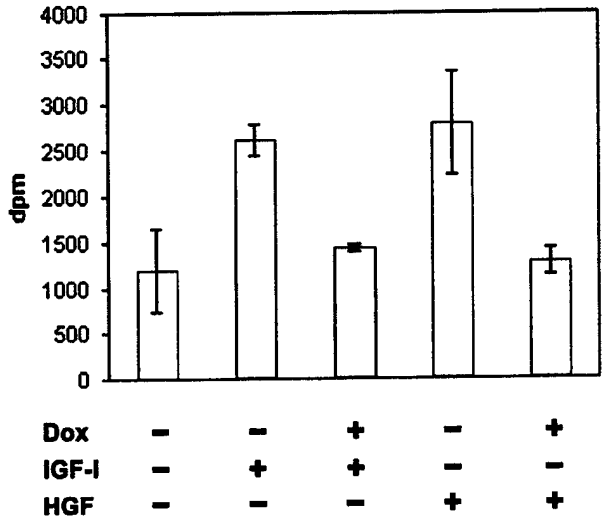

Figure 3. Schwannomin inhibits RT4 schwannoma proliferation in response to IGF-I and HGF. Ten thousand Tet-on RT4 NF2.17 cells were seeded in quadruplicate 24-well plates and serum-starved for 24 h prior to the addition of 100 ng/ml IGF-I or 200 ng/ml HGF overnight either in presence or absence of doxycycline to induce schwannomin expression. Thymidine incorporation was measured after 4 h. Mean and SD are shown for each condition.

Stat3 was observed after 24 h of induced schwannomin isoform I expression in Tet-on RT4 NF2.17 cells (Fig. 4A). We also showed that IGF-I phosphorylates Stat3 in Tet-off STS26T NF2i1 cells and that schwannomin isoform I expression in these cells inhibited Stat3 phosphorylation to the level observed in untreated cells (Fig. 4B). We then tested whether IGF-I-mediated SIE activity could be inhibited by schwannomin in STS26T cells. In these experiments, SIE activation increased in response to increasing IGF-I concentrations (0, 20 and 40 ng/ml) in the absence of schwannomin, but when schwannomin was expressed no increased SIE activation was observed (Fig. 5). We conclude that STAT activation by the STAT activator, IGF-I, is inhibited by schwannomin, and that schwannomin lies in a signaling pathway between the IGF-I receptor and Stat3.

Schwannomin inhibits phosphorylation of Stat5

To determine whether schwannomin inhibits only STATs that activate SIE, we also assessed the ability of schwannomin isoform I to inhibit Stat5 phosphorylation in RT4 cells. For these experiments, we employed RT4 cells that inducibly express schwannomin isoform I in response to doxycycline treatment. Increased expression of schwannomin isoform I resulted in decreased abundance of phosphorylated Stat5 (Fig. 6A, left). However, when we used a matched Tet-on RT4 inducible cell line expressing schwannomin isoform I containing the Q538P mutation, we did not observe any decrease in Stat5 phosphorylation (Fig. 6A, right). We tested the ability of this schwannomin isoform I mutant to bind HRS and found that the Q538P mutation abolished the HRS interaction (Fig. 6B).

DISCUSSION

The *NF2* gene is one of the most commonly mutated genes in human benign brain tumors, including schwannomas and meningiomas. Despite the identification of several proteins that interact with the NF2 tumor suppressor schwannomin, a single schwannomin-regulated pathway altered by *NF2* mutation to cause tumorigenesis has not been defined.

In previous studies we identified HRS as a schwannomin interacting protein (27). Two intriguing features about HRS suggested that HRS could regulate pathways that lead to STAT activation and, being a schwannomin interactor, that schwannomin might regulate these HRS actions. Firstly, HRS facilitates trafficking of ubiquitinated RTKs to the degradation pathway (31–33) and, secondly, HRS interacts with the signal transduction adapter molecule STAM, which is a ubiquitous protein involved in cytokine-mediated signal transduction (34,35). While the action of STAM on STATs has not been studied, it has been shown that STAM interaction with Janus kinases causes elevated c-*myc* induction and DNA synthesis and that HRS can inhibit STAM activation (34,35). Like HRS, STAM also possesses a ubiquitin-interacting motif (UIM) and may participate in HRS-mediated trafficking of RTKs (41). Since STAT proteins are often found overexpressed in a variety of tumors types, including ovary and breast tumor cells (42–44) and Stat1 and Stat3 are overexpressed in meningiomas (45), we investigated schwannomin and HRS ability to inhibit STAT signaling in human and rat schwannoma cell lines.

The STAT proteins comprise a family of proteins that are activated upon ligand binding by cytokine receptors or RTKs, sometimes requiring Janus kinases (Jaks) (46). Once phosphorylated, STATs then homo- or heterodimerize and translocate to the nucleus where they function as transcription factors, interacting with specific inducible elements. We chose to investigate the ability of schwannomin to inhibit the activation of the *sis* inducible element SIE, which is activated by Stat1 and Stat3, and the S3 inducible element, which is activated by Stat3. We now show that both schwannomin and HRS inhibit SIE and S3 activation.

Overexpression of increasing dosages of schwannomin isoforms or HRS in STS26T cells strongly inhibited SIE and S3 activation. Inducible expression of schwannomin in RT4 cells and transiently expressed schwannomin in STS26T cells decreased the abundance of nuclear Stat3. The abundance of phosphorylated Stat3 was decreased when we inducibly overexpressed schwannomin in RT4 or STS26T cells. The Q538P schwannomin mutation impaired the ability of schwannomin isoform II to inhibit SIE activation. To determine whether schwannomin might inhibit other STATs that do not activate SIE, we also investigated the effect of schwannomin on Stat5. Induced schwannomin expression inhibited Stat5 phosphorylation. In addition, Q538P-mutated schwannomin isoform I, which does not interact with HRS, did not inhibit the phosphorylation of Stat5, when inducibly expressed. These findings are consistent with a requirement for HRS interaction by schwannomin for schwannomin to inhibit STAT activation.

IGF-I is established as an activator of Stat3 in a variety of cell types, and stimulates proliferation of Schwann cells (37–39). We verified that both IGF-I and HGF induce proliferation of RT4 cells and demonstrated that schwannomin overexpression

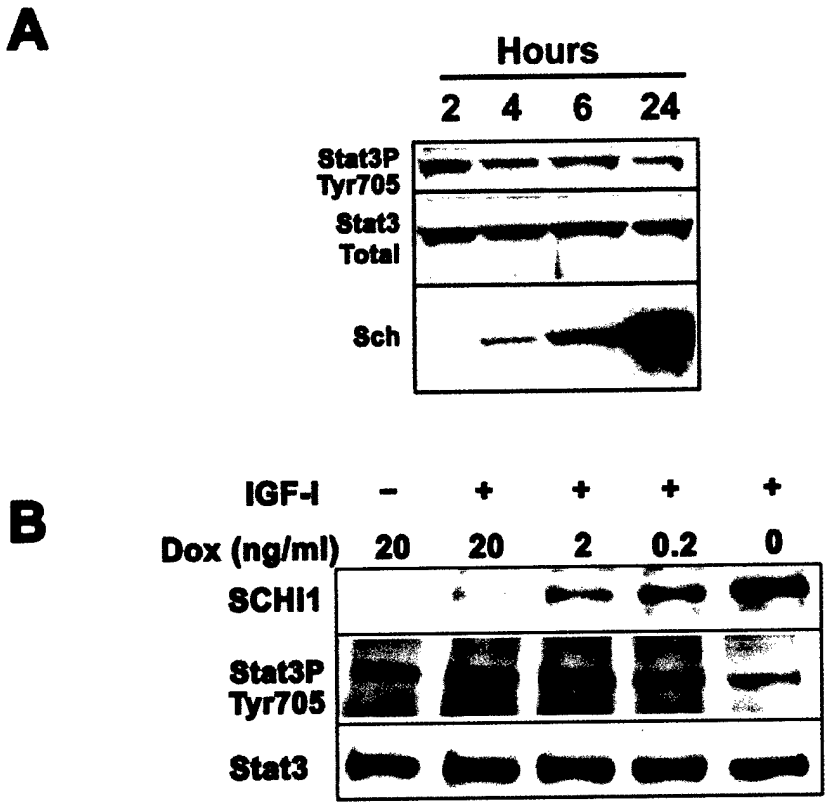

Figure 4. Schwannomin inhibits Stat3 phosphorylation in RT4 and STS26T cells. (**A**) Induction of schwannomin results in decreased Stat3 activity. Subconfluent schwannomin-inducible Tet-on RT4 NF2.17 cell cultures were treated with doxycycline for 2, 4, 6 and 24 h prior to harvest. Protein extracts were subjected to immunoblot analysis using antibodies that recognize Stat3 phosphorylated on tyrosine 705 (Stat3p) or total Stat3. At 24 h, decreased Stat3 activity in response to schwannomin induction was indicated by lower abundance of phosphorylated Stat3, while total Stat3 remained unchanged. (**B**) Schwannomin-inducible Tet-off STS26T NF2i1 cell cultures were treated with the indicated amounts of doxycycline for 2 days. Cells were serum-starved overnight (same dox conditions) and then treated with 50 ng/ml IGF-I (or diluent) for 10 min before extraction. The addition of IGF-I increased the abundance of phosphorylated Stat3. In cells expressing the greatest amount of schwannomin, the level of phosphorylated Stat3 was reduced to amounts seen in cells that were not stimulated with IGF-I. Schwannomin was detected in (A) using antibody WA30 and in (B) using antibody ab2781.

can inhibit SIE activation stimulated by IGF-I treatment. Both schwannomin isoforms I and II were able to inhibit STAT activation. Previous studies using model systems to compare the schwannomin isoforms functionally have demonstrated that, unlike schwannomin isoform I, schwannomin isoform II had no ability to alter Schwann cell proliferation, tumor growth or cytoskeletal reorganization (21,23,47). The schwannomin isoforms are highly conserved evolutionarily, including the splice signals, suggesting that both isoforms have important cellular functions (48,49). STATs are powerful mediators of signal transduction and while when previously used *in vitro* systems they did not establish a link between isoform II and tumorigenesis, both schwannomin isoforms may have some significant role in the regulation of proliferative pathways at the organismal level. Alternatively, it is possible that the ability of schwannomin and HRS to inhibit STAT activation reflects another function of these proteins not related to the inhibition of cell proliferation.

A variety of receptors that activate Stat3 also activate Stat5. The ability of schwannomin to inhibit both Stat3 and Stat5 activation is consistent with the ability of schwannomin to function as a growth regulator by inhibiting a wide variety of signals that activate multiple STATs. The actions by schwannomin on STATs may involve HRS and its ability to traffic STAT-activating cell surface receptors to the lysosome (32,33). HRS overexpression in RT4 cells strongly alters the localization of EGF receptor in RT4 cells (Scoles, Gutmann and Pulst, manuscript in preparation). Recently, we have shown that schwannomin acts upstream of HRS and that HRS is required for schwannomin-mediated inhibition of proliferation in mouse embryo fibroblasts (50). Consistent with this finding, we could show no synergistic effect on STAT inhibition caused by the expression of both HRS and schwannomin (data not shown). This finding is also consistent with the inability of Q538 schwannomin to inhibit STAT activation caused by loss of HRS interaction. However, we have not yet proven that STAT inhibition by schwannomin involves HRS-mediated receptor trafficking. In an effort to demonstrate a schwannomin link to STAM, we investigated the ability of schwannomin to inhibit c-fos expression, but we were unable to reproducibly show that

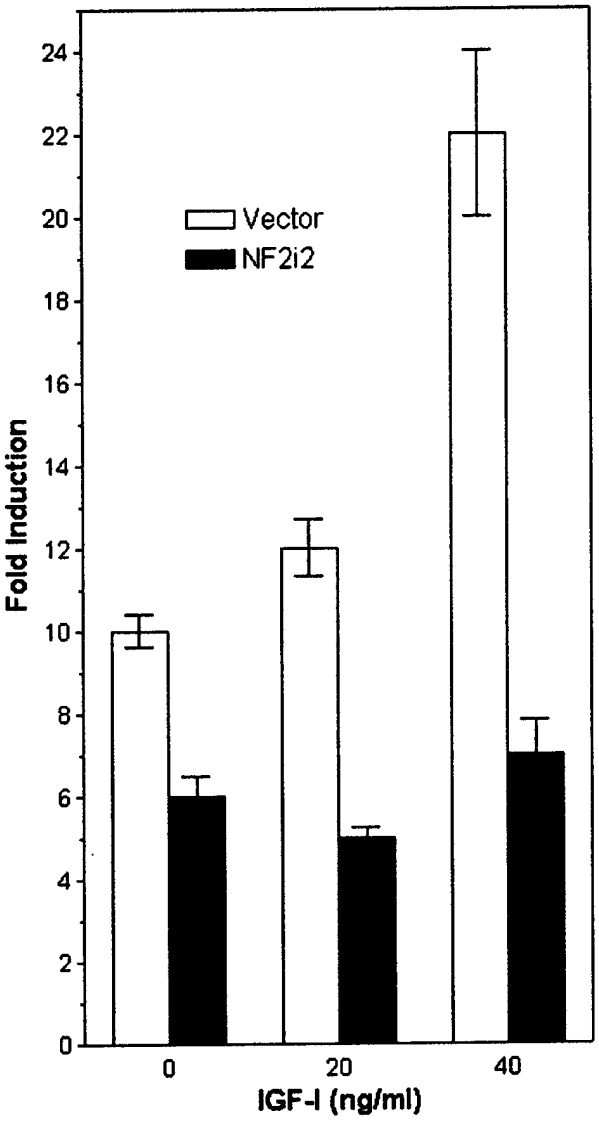

Figure 5. Schwannomin inhibits IGF-I mediated activation of the SIE promoter element for STAT signaling. STS26T cells were transfected with pLukTKSIE and 9 μg expression vector with no insert, or pLukTKSIE and 9 μg plasmid expressing schwannomin isoform II. Cells were treated with the indicated amounts of IGF-I before assaying for luciferase activity. Fold induction is relative to control experiments detecting pLukTK activation. For this experiment, STS26T cells were transiently transfected and luciferase reporter activities were measured as light emission with a luminometer. The results shown are mean ± SD of triplicate measures.

schwannomin overexpression affected c-fos abundance. Further work will be required to elucidate the mechanism by which schwannomin inhibits STAT activation.

Regulation of Stat3 by schwannomin may be related to Rac signaling. Recent studies have shown that schwannomin can be phosphorylated by p21-activated kinase (PAK2) in response to activated Rac1 (24–26). In Schwann cells, dominant inhibitory Rac1 blocks IGF-I-mediated motility (51) and constitutively active Rac1 can directly activate Stat3, leading to Stat3 nuclear translocation (52,53). Our results demonstrating schwannomin suppression of Stat3 are consistent with a relationship to Rac signaling and suggest one possible mechanism by which schwannomin can inhibit Rac-mediated Stat3 activation. The finding that schwannomin and its interacting protein HRS both strongly suppress Stat3 signaling is significant to potential treatment strategies for tumors in NF2, since constitutive activation of Stat3 by mutation is oncogenic (54). Treatments that target Stat3 and other STAT proteins may prove to be highly effective at inhibiting the growth of NF2-related tumors.

MATERIALS AND METHODS

Antibodies

The Xpress epitope tag encoded on pcDNA3.1his was detected with anti-Xpress antibody (R91025, Invitrogen). Polyclonal chicken anti-schwannomin antibody ab2781 was raised against schwannomin residues 528–541 (YMEKSKHLQEQLNE) and affinity purified. Polyclonal rabbit anti-merlin antibody WA30 was raised against schwannomin residues 192–209 (YAEHRGRARDEAEMEYLK) as previously described (55). Phosphorylated Stat3 was detected on immunoblots using monoclonal anti-phospho-Stat3 (Tyr705) antibody (9131, Cell Signaling Technology). Total Stat3 was detected on immunoblots using a rabbit polyclonal Stat3 antibody (9132, New England Biolabs) and was detected for immunofluorescent localization using a rabbit polyclonal Stat3 antibody (sc482, Santa Cruz). Phosphorylated Stat5 was detected using monoclonal anti-phospho-Stat5 (Tyr694) antibody (9351, New England Biolabs) and total Stat5 was detected using a monoclonal anti-Stat5 antibody (S21520, Transduction Laboratories). All secondary antibodies used in the study were purchased from Jackson ImmunoResearch Laboratories.

Constructs

The pcDNA3.1hisB-NF2i2 construct was generated by excising the NF2i2 fragment from pGBT9-NF2i2 [previously described (22)] with *Sma*I and *Sal*I and ligating it with pcDNA3.1hisB (Invitrogen) digested with *Eco*RV and *Xho*I. The pcDNA3.1hisB–NF2i1 construct was made by removing the C-terminal half of the NF2i2 gene from pcDNA3.1hisB–NF2i2 with *Xho*I and *Xba*I and ligating in its place the C-terminal fragment of the NF2i1 gene removed from pGBT9–NF2i1 with the same two restriction enzymes. To construct pcDNA3.1hisB–NF2i2 (Q538P), the full-length mutant NF2 gene was removed from the pGBT9–NF2i2 (Q538P) [previously described (22)] with *Sma*I and *Sal*I and ligated with pcDNA3.1hisB digested with *Eco*RV and *Xho*I. pcDNA3.1hisB–HRSi1 was made by excising the HRSi1 fragment from pGAD10–HRSi1 [previously described (22)] with *Sal*I and ligating in the *Xho*I site of pcDNA3.1hisB. The plasmids pGBT9–NF2i1 and pGAD10–HRS were described previously (22). To construct pGBT9–NF2i1 (Q538P), a portion of the mutant NF2 gene containing Q538P was removed from pGBT9–NF2i2 (Q538P) with *Hpa*I and *Stu*I and ligated in place of the corresponding portion removed from

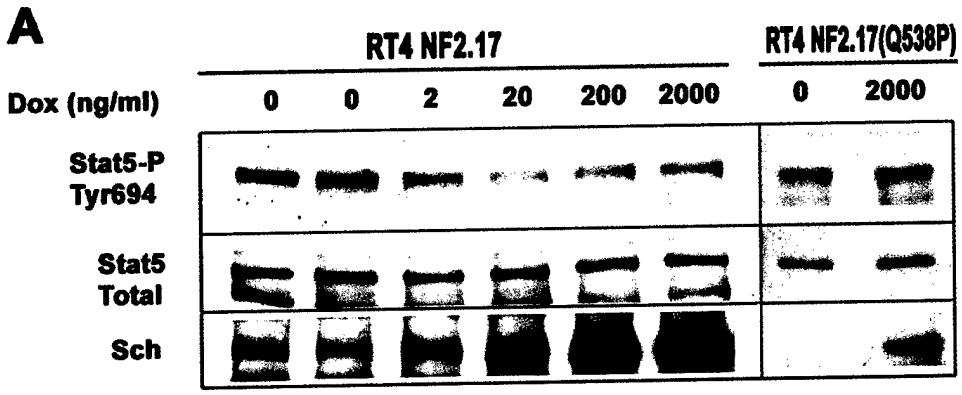

B

Schwannomin isofrom I with mutation Q538P does not bind HRS

Interaction			Plate Assay	β-Galactosidase Units
pGBT9		pGAD10		
NF2i1	*vs*	HRS		214.3 ± 4.1
NF2i1(Q538P)	*vs*	HRS		1.19 ± 0.093
NF2i1	*vs*	Vector		0.17 ± 0.069
NF2i1(Q538P)	*vs*	Vector		0.28 ± 0.023
Vector	*vs*	HRS		0.36 ± 0.023

Figure 6. Schwannomin inhibits STAT5 phosphorylation in Tet-on RT4 NF2.17 cells. (**A**) Left panel: seven identical cultures of Tet-on RT4 NF2.17 cells were treated with the indicated concentrations of doxycycline (ng/ml) for 24 h. Protein extracts were subjected to immunoblot analysis using antibodies that recognize Stat5 phosphorylated on tyrosine 694 (Stat5p), total Stat5 or schwannomin detected with antibody ab2781. A reduced abundance of Stat5p was observed for all treatments when doxycycline was used. Note that the treatment without doxycycline is replicated. Right panel: no reduction of Stat5 phosphorylation was observed upon expression of schwannomin mutated at position Q538P. (**B**) Yeast two-hybrid tests of interaction demonstrated that schwannomin isoform I with the mutation Q538P has considerably reduced HRS binding affinity compared with wild-type schwannomin isoform I.

pGBT9–NF2i1 with the same restriction enzymes. The pRevTet-Off–NF2i1 construct was made by excising the NF2i1 insert from pcDNA3.1hisB–NF2i1 with *Bam*HI and ligating in to the *Bam*HI site of pRevTet-Off (Clontech).

Luciferase assays

STS26T or RT4 cells were grown in DMEM containing 10% FBS. Transfections were conducted using Superfect as recommended by the vendor (Qiagen). Total transfected DNA was 16.7 μg on a 100 mm dish, including 7.1 μg of luciferase reporter plasmid (pLucTK, pLukTKS3 or pLucTKSIE), 0.6 μg pcDNA3.1his–LacZ internal control plasmid (Invitrogen) and 9 μg total expression plasmid [pcDNA3.1his, pcDNA3.1his–NF2i1, pcDNA3.1his–NF2i2, pcDNA3.1his–NF2i2 (L46R), pcDNA3.1his–NF2i2 (Q538P), pcDNA3.1his–NF2N (1-305), pcDNA3.1his–NF2i1C (299–595), pcDNA3.1his-HRSi1]. After 48 h of transfection, cells were washed twice with Dulbecco's phosphate buffered saline (DPBS, Sigma), removed with 0.5% trypsin, 5.3 mM EDTA and trypsin was neutralized with growth media and cells were pelleted. When cells were stimulated with IGF-I, twice the cell volume was used for each treatment (2 × 100 mm dishes). After transfection cells were recovered in media containing 10% serum overnight, then were serum-starved for 24 h before being stimulated with IGF-I at the indicated concentrations for an additional 6 h. Cytosolic extracts were used for luciferase assays (Luciferase Assay System, Promega). β-Galactosidase activity was determined by the liquid assay method as described below for yeast extracts, with chloroform omitted. Luciferase activity = [counts

luciferase/OD_{420}]. The luciferase reporter system was a gift from Richard Jove, University of South Florida.

Yeast two-hybrid tests of interaction

The methods for testing protein–protein interactions were described previously (22,27,28). The yeast strain Y190 was co-transformed with pGBT9 and pGAD10 constructs as indicated and grown on SC media with leucine and tryptophan dropped out and with 2% glucose. β-Galactosidase production was assayed by incubating freeze-fractured colonies on nitrocellulose in Z-buffer (60 mM Na_2HPO_4, 40 mM NaH_2PO_4, 10 mM KCl, 1 mM $MgSO_4$, pH 7.0, 0.03 mM β-mercaptoethanol and 2.5 μM X-gal) at 37°C. Liquid assays for β-galactosidase were conducted by incubating yeast extracted in Z-buffer and 5% chloroform with 0.6 mg/ml *o*-nitrophenyl-beta-D-galactopyranoside for 1 h. Color intensity depends on the amount of β-galactosidase present and is measured spectrophotometrically at 420 nm. β-Galactosidase units = $1000 \times [OD_{420}/(OD_{600} \times \text{time} \times \text{volume})]$.

Cell lines

The Schwann-like STS26T cell line is derived from a human malignant schwannoma (56). The schwannomin-inducible Tet-off RT4 NF2.17 cell line was described previously (15). The schwannomin-inducible Tet-off STS26T cell line was generated by using the RevTet-Off vector system (Clontech) as follows: STS26T cells were infected with retrovirus made from packaging cell line PT67 stably transfected with pRevTet-Off (G418, Invitrogen). Resistant Tet-Off STS26T cells were then trypsinized, diluted 40 000 times and plated in three 96-well plates (these dilution conditions allowed for an average of one cell per well). After cells reached confluency, each plate was seeded in triplicate [one pair of plates for dox/no dox comparisons, grown in black opaque tissue culture plates (Greiner Bio-One) and a third for propagation of lines]. Each pair of plates was transiently transfected (Superfect, Qiagen) with pRevTRE-Luc and then one of each pair was treated with doxycycline and the other with no doxycycline. Luciferase was detected in the plates using a 6-detector 1450 Microbeta Liquid Scintillation Counter (Perkin Elmer) with coincidence counting deactivated and Luciferase Assay Reagent (Promega). Of the <288 lines screened, we propagated 24 of the best lines and we assayed for induction of transiently transfected pRevTRE-Luc activation using a luminometer. The line best inducing luciferase with minimal detected reporter leak was then infected by retrovirus made from PT67 stably selected with RevTRE-NF2i1 and cells were placed under neomycin/hygromycin B selection (Invitrogen). Forty-eight colonies of Tet-off STS26T NF2i1 cells were collected by ring-cloning and tested for doxycycline inducible schwannomin expression by immunoblotting with antibody ab2781. The line used in our study is Tet-off STS26T NF2i1.F9.3 and is one of seven retained.

Immunofluorescence

STS26T cells (30 000 cells per well in four-well slides) were grown in DMEM with 10% FBS overnight. Cells were labeled for immunofluorescence as previously described (22,57). The primary antibody dilutions were 5 μg/ml anti-Stat3, 5 μg/ml anti-schwannomin ab1781, or 1:500 dilution anti-Xpress. Primary antibodies were incubated 60 min at 37°C. For the co-detection of Xpress-schwannomin and Stat3, cells were incubated with FITC-conjugated affinity purified goat anti-rabbit IgG or rhodamine-conjugated affinity purified goat anti-mouse IgG for 1 h at room temperature. For the detection of Stat3 in RT4 NF2.17 cells, cells were plated on poly-lysine-coated cover glasses and detected using rhodamine-conjugated affinity purified goat anti-rabbit IgG. After antibody incubations, cells were washed six times in cold DPBS and mounted. For Figure 2A–F, fluorescent confocal microscopy was performed using a Zeiss LSM 310 confocal microscope. Fluorescein was visualized with a BP485/20/BP520–560 excitation/emission filter set (Zeiss filter set 17) and scanning was done with a 488 nm argon laser and a BP520–560 barrier filter. Rhodamine visualization was done with a BP515–560/LP590 excitation/emission filter set (Zeiss filter set 15) and scanning performed with a 543 nm HeNe laser and an LP590 nm barrier filter. For Figure 2G–J, fluorescent confocal microscopy was performed using a Leica TCS SP confocal microscope. Rhodamine was excited with a HeNe laser at 568 nm with emission set to a range of 596–671 nm.

Proliferation assays

Proliferation experiments were performed after an overnight induction in 1 μg/ml doxycycline after a 24 h serum starvation period. IGF-I (100 ng/ml) or HGF (200 ng/ml) was added for the 4 h thymidine incorporation period. Thymidine incorporation was performed as previously described (47). Each condition was performed in six duplicate wells.

Stat phosphorylation assay

For the analysis of Stat3 phosphorylation in Tet-off STS26T NF2il cells, the cells were equally-plated in DMEM containing 10% FBS prior to the addition of 100 μl of a 100x solution of doxycycline (to maintain the diluent background, the dilution series was made prior to the addition). After two days induction cells were serum-starved overnight then treated with 50 ng/ml IGF-I for 10 min. For the analysis of Stat3 phosphorylation in Tet-on RT4 NF2.17 cells, the cells were equally-plated in DMEM containing 10% fetal bovine serum (FBS) prior to the addition of 1 μg/ml doxycycline for 2, 4, 6 and 24 h. For the analysis of Stat5 in Tet-on RT4–NF2.17, or RT4–NF2.17(Q538P) cells, the cells were equally-plated in DMEM containing 10% FBS prior to the addition of 100 μl of a 100× solution of doxycycline and incubated for 24 h. Cells were harvested on ice in Cell Lysis Buffer (Cell Signaling Technology) and equal amounts of protein were loaded onto 4–15% SDS–PAGE gels and immunoblotting was performed.

ACKNOWLEDGEMENTS

We thank Richard Jove (University of South Florida) for providing luciferase reporter plasmids and Matt Schibler (UCLA Brain Institute), Kolja Wawrowski and Kamlesh Asotra (Cedars-Sinai Medical Center) for assistance with confocal microscopy. We thank Richard Deem for assistance

on luciferase detections in the microtiter plate format. This work was supported by the Carmen and Louis Warschaw Endowment Fund and FRIENDs of Neurology. Support was also provided by grants NS01428-01A1 from the National Institutes of Health (NIH) and DAMD17-99-1-9548 from the Department of Defense (DoD) to S.M.P., NS35848 from NIH to D.H.G., NS10524-02 from NIH and DAMD17-00-1-0553 from DoD to D.R.S. and a shared equipment grant no. 1S10-RR13717 from NIH.

REFERENCES

1. Sainz, J., Huynh, D.P., Figueroa, K., Ragge, N.K., Baser, M.E. and Pulst, S.M. (1994) Mutations of the neurofibromatosis type 2 gene and lack of the gene product in vestibular schwannomas. *Hum. Mol. Genet.*, **3**, 885–891.
2. Ruttledge, M.H., Sarrazin, J., Rangaratnam, S., Phelan, C.M., Twist, E., Merel, P., Delattre, O., Thomas, G., Nordenskjold, M., Collins, V.P. *et al.* (1994) Evidence for the complete inactivation of the NF2 gene in the majority of sporadic meningiomas. *Nat. Genet.*, **6**, 180–184.
3. Rubio, M.P., Correa, K.M., Ramesh, V., MacCollin, M.M., Jacoby, L.B., von Deimling, A., Gusella, J.F. and Louis, D.N. (1994) Analysis of the neurofibromatosis 2 gene in human ependymomas and astrocytomas. *Cancer Res.*, **54**, 45–47.
4. Huynh, D.P., Mautner, V., Baser, M.E., Stavrou, D. and Pulst, S.M. (1997) Immunohistochemical detection of schwannomin and neurofibromin in vestibular schwannomas, ependymomas and meningiomas. *J. Neuropathol. Exp. Neurol.*, **56**, 382–390.
5. Trofatter, J.A., MacCollin, M.M., Rutter, J.L., Murrell, J.R., Duyao, M.P., Parry, D.M., Eldridge, R., Kley, N., Menon, A.G., Pulaski, K. *et al.* (1993) A novel moesin-, ezrin-, radixin-like gene is a candidate for the neurofibromatosis 2 tumor suppressor. *Cell*, **75**, 826.
6. Rouleau, G.A., Merel, P., Lutchman, M., Sanson, M., Zucman, J., Marineau, C., Hoang-Xuan, K., Demczuk, S., Desmaze, C., Plougastel, B. *et al.* (1993) Alteration in a new gene encoding a putative membrane-organizing protein causes neuro-fibromatosis type 2. *Nature*, **363**, 515–521.
7. Bretscher, A., Chambers, D., Nguyen, R. and Reczek, D. (2000) ERM-Merlin and EBP50 protein families in plasma membrane organization and function. *A. Rev. Cell. Devl. Biol.*, **16**, 113–143.
8. Jannatipour, M., Dion, P., Khan, S., Jindal, H., Fan, X., Laganiere, J., Chishti, A.H. and Rouleau, G.A. (2001) Schwannomin isoform-1 interacts with syntenin via PDZ domains. *J. Biol. Chem.*, **276**, 33093–33100.
9. Goutebroze, L., Brault, E., Muchardt, C., Camonis, J. and Thomas, G. (2000) Cloning and characterization of SCHIP-1, a novel protein interacting specifically with spliced isoforms and naturally occurring mutant NF2 proteins. *Mol. Cell. Biol.*, **20**, 1699–1712.
10. Sainio, M., Zhao, F., Heiska, L., Turunen, O., den Bakker, M., Zwarthoff, E., Lutchman, M., Rouleau, G.A., Jaaskelainen, J., Vaheri, A. *et al.* (1997) Neurofibromatosis 2 tumor suppressor protein colocalizes with ezrin and CD44 and associates with actin-containing cytoskeleton. *J. Cell. Sci.*, **110** (Pt 18), 2249–2260.
11. Reczek, D., Berryman, M. and Bretscher, A. (1997) Identification of EBP50: A PDZ-containing phosphoprotein that associates with members of the ezrin-radixin-moesin family. *J. Cell. Biol.*, **139**, 169–179.
12. Murthy, A., Gonzalez-Agosti, C., Cordero, E., Pinney, D., Candia, C., Solomon, F., Gusella, J. and Ramesh, V. (1998) NHE-RF, a regulatory cofactor for Na(+)-H+ exchange, is a common interactor for merlin and ERM (MERM) proteins. *J. Biol. Chem.*, **273**, 1273–1276.
13. Maeda, M., Matsui, T., Imamura, M. and Tsukita, S. (1999) Expression level, subcellular distribution and rho-GDI binding affinity of merlin in comparison with Ezrin/Radixin/Moesin proteins. *Oncogene*, **18**, 4788–4797.
14. Gronholm, M., Sainio, M., Zhao, F., Heiska, L., Vaheri, A. and Carpen, O. (1999) Homotypic and heterotypic interaction of the neurofibromatosis 2 tumor suppressor protein merlin and the ERM protein ezrin. *J. Cell. Sci.*, **112** (Pt 6), 895–904.
15. Gutmann, D.H., Haipek, C.A., Burke, S.P., Sun, C.X., Scoles, D.R. and Pulst, S.M. (2001) The NF2 interactor, hepatocyte growth factor-regulated tyrosine kinase substrate (HRS), associates with merlin in the 'open' conformation and suppresses cell growth and motility. *Hum. Mol. Genet.*, **10**, 825–834.
16. Gonzalez-Agosti, C., Wiederhold, T., Herndon, M.E., Gusella, J. and Ramesh, V. (1999) Interdomain interaction of merlin isoforms and its influence on intermolecular binding to NHE-RF. *J. Biol. Chem.*, **274**, 34438–34442.
17. Scoles, D.R., Baser, M.E. and Pulst, S.M. (1996) A missense mutation in the neurofibromatosis 2 gene occurs in patients with mild and severe phenotypes. *Neurology*, **47**, 544–546.
18. Fernandez-Valle, C., Tang, Y., Ricard, J., Rodenas-Ruano, A., Taylor, A., Hackler, E., Biggerstaff, J. and Iacovelli, J. (2002) Paxillin binds schwannomin and regulates its density-dependent localization and effect on cell morphology. *Nat. Genet.*, **31**, 354–362.
19. Xu, H.M. and Gutmann, D.H. (1998) Merlin differentially associates with the microtubule and actin cytoskeleton. *J. Neurosci. Res.*, **51**, 403–415.
20. Pelton, P.D., Sherman, L.S., Rizvi, T.A., Marchionni, M.A., Wood, P., Friedman, R.A. and Ratner, N. (1998) Ruffling membrane, stress fiber, cell spreading and proliferation abnormalities in human Schwannoma cells. *Oncogene*, **17**, 2195–2209.
21. Bashour, A.M., Meng, J.J., Ip, W., MacCollin, M. and Ratner, N. (2002) The neurofibromatosis type 2 gene product, merlin, reverses the F-actin cytoskeletal defects in primary human Schwannoma cells. *Mol. Cell. Biol.*, **22**, 1150–1157.
22. Scoles, D.R., Huynh, D.P., Morcos, P.A., Coulsell, E.R., Robinson, N.G., Tamanoi, F. and Pulst, S.M. (1998) Neurofibromatosis 2 tumour suppressor schwannomin interacts with betaII-spectrin. *Nat. Genet.*, **18**, 354–359.
23. Gutmann, D.H., Sherman, L., Seftor, L., Haipek, C., Hoang Lu, K. and Hendrix, M. (1999) Increased expression of the NF2 tumor suppressor gene product, merlin, impairs cell motility, adhesionand spreading. *Hum. Mol. Genet.*, **8**, 267–275.
24. Shaw, R.J., Paez, J.G., Curto, M., Yaktine, A., Pruitt, W.M., Saotome, I., O'Bryan, J.P., Gupta, V., Ratner, N., Der, C.J. *et al.* (2001) The Nf2 tumor suppressor, merlin, functions in Rac-dependent signaling. *Devl. Cell.*, **1**, 63–72.
25. Xiao, G.H., Beeser, A., Chernoff, J. and Testa, J.R. (2002) p21-activated kinase links Rac/Cdc42 signaling to merlin. *J. Biol. Chem.*, **277**, 883–886.
26. Kissil, J.L., Johnson, K.C., Eckman, M.S. and Jacks, T. (2002) Merlin phosphorylation by p21-activated kinase 2 and effects of phosphorylation on merlin localization. *J. Biol. Chem.*, **277**, 10394–10399.
27. Scoles, D.R., Huynh, D.P., Chen, M.S., Burke, S.P., Gutmann, D.H. and Pulst, S.M. (2000) The neurofibromatosis 2 tumor suppressor protein interacts with hepatocyte growth factor-regulated tyrosine kinase substrate. *Hum. Mol. Genet.*, **9**, 1567–1574.
28. Scoles, D.R., Chen, M. and Pulst, S.M. (2002) Effects of Nf2 missense mutations on schwannomin interactions. *Biochem. Biophys. Res. Commun.*, **290**, 366–374.
29. Komada, M., Masaki, R., Yamamoto, A. and Kitamura, N. (1997) Hrs, a tyrosine kinase substrate with a conserved double zinc finger domain, is localized to the cytoplasmic surface of early endosomes. *J. Biol. Chem.*, **272**, 20538–20544.
30. Gaullier, J.M., Simonsen, A., D'Arrigo, A., Bremnes, B., Stenmark, H. and Aasland, R. (1998) FYVE fingers bind PtdIns(3)P. *Nature*, **394**, 432–433.
31. Shih, S.C., Katzmann, D.J., Schnell, J.D., Sutanto, M., Emr, S.D. and Hicke, L. (2002) Epsins and Vps27p/Hrs contain ubiquitin-binding domains that function in receptor endocytosis. *Nat. Cell. Biol.*, **4**, 389–393.
32. Raiborg, C., Bache, K.G., Gillooly, D.J., Madshus, I.H., Stang, E. and Stenmark, H. (2002) Hrs sorts ubiquitinated proteins into clathrin-coated microdomains of early endosomes. *Nat. Cell. Biol.*, **4**, 394–398.
33. Lloyd, T.E., Atkinson, R., Wu, M.N., Zhou, Y., Pennetta, G. and Bellen, H.J. (2002) Hrs regulates endosome membrane invagination and tyrosine kinase receptor signaling in Drosophila. *Cell*, **108**, 261–269.
34. Asao, H., Sasaki, Y., Arita, T., Tanaka, N., Endo, K., Kasai, H., Takeshita, T., Endo, Y., Fujita, T. and Sugamura, K. (1997) Hrs is associated with STAM, a signal-transducing adaptor molecule. Its suppressive effect on cytokine-induced cell growth. *J. Biol. Chem.*, **272**, 32785–32791.
35. Takeshita, T., Arita, T., Higuchi, M., Asao, H., Endo, K., Kuroda, H., Tanaka, N., Murata, K., Ishii, N. and Sugamura, K. (1997) STAM, signal transducing adaptor molecule, is associated with Janus kinases and involved in signaling for cell growth and c-myc induction. *Immunity*, **6**, 449–457.
36. Turkson, J., Bowman, T., Garcia, R., Caldenhoven, E., De Groot, R.P. and Jove, R. (1998) Stat3 activation by Src induces specific gene

regulation and is required for cell transformation. *Mol. Cell. Biol.*, **18**, 2545–2552.
37. Schumacher, M., Jung-Testas, I., Robel, P. and Baulieu, E.E. (1993) Insulin-like growth factor I: a mitogen for rat Schwann cells in the presence of elevated levels of cyclic AMP. *Glia*, **8**, 232–240.
38. Cheng, H.L., Russell, J.W. and Feldman, E.L. (1999) IGF-I promotes peripheral nervous system myelination. *Ann. NY Acad. Sci.*, **883**, 124–130.
39. Zong, C.S., Chan, J., Levy, D.E., Horvath, C., Sadowski, H.B. and Wang, L.H. (2000) Mechanism of STAT3 activation by insulin-like growth factor I receptor. *J. Biol. Chem.*, **275**, 15099–15105.
40. Krasnoselsky, A., Massay, M.J., DeFrances, M.C., Michalopoulos, G., Zarnegar, R. and Ratner, N. (1994) Hepatocyte growth factor is a mitogen for Schwann cells and is present in neurofibromas. *J. Neurosci.*, **14**, 7284–7290.
41. Lohi, O. and Lehto, V.P. (2001) STAM/EAST/Hbp adapter proteins—integrators of signalling pathways. *FEBS Lett.*, **508**, 287–290.
42. Garcia, R., Bowman, T.L., Niu, G., Yu, H., Minton, S., Muro-Cacho, C.A., Cox, C.E., Falcone, R., Fairclough, R., Parsons, S. *et al.* (2001) Constitutive activation of Stat3 by the Src and JAK tyrosine kinases participates in growth regulation of human breast carcinoma cells. *Oncogene*, **20**, 2499–2513.
43. Buettner, R., Mora, L.B. and Jove, R. (2002) Activated STAT signaling in human tumors provides novel molecular targets for therapeutic intervention. *Clin. Cancer Res.*, **8**, 945–954.
44. Huang, M., Page, C., Reynolds, R.K. and Lin, J. (2000) Constitutive activation of stat 3 oncogene product in human ovarian carcinoma cells. *Gynecol. Oncol.*, **79**, 67–73.
45. Magrassi, L., De-Fraja, C., Conti, L., Butti, G., Infuso, L., Govoni, S. and Cattaneo, E. (1999) Expression of the JAK and STAT superfamilies in human meningiomas. *J. Neurosurg.*, **91**, 440–446.
46. Darnell, J.E. Jr (1997) STATs and gene regulation. *Science*, **277**, 1630–1635.
47. Sherman, L., Xu, H.M., Geist, R.T., Saporito-Irwin, S., Howells, N., Ponta, H., Herrlich, P. and Gutmann, D.H. (1997) Interdomain binding mediates tumor growth suppression by the *NF2* gene product. *Oncogene*, **15**, 2505–2509.
48. Huynh, D.P., Nechiporuk, T. and Pulst, S.M. (1994) Alternative transcripts in the mouse neurofibromatosis type 2 (*NF2*) gene are conserved and code for schwannomins with distinct C-terminal domains. *Hum. Mol. Genet.*, **3**, 1075–1079.
49. Jacoby, L.B., MacCollin, M., Louis, D.N., Mohney, T., Rubio, M.P., Pulaski, K., Trofatter, J.A., Kley, N., Seizinger, B., Ramesh, V. *et al.* (1994) Exon scanning for mutation of the *NF2* gene in schwannomas. *Hum. Mol. Genet.*, **3**, 413–419.
50. Sun, C.-X., Haipek, C., Scoles, D.R., Pulst, S.M., Giovannini, M., Komada, M. and Gutmann, D.H. (2002) Functional analysis of the relationship between the neurofibromatosis 2 tumor suppressor and its binding partner, hepatocyte growth factor-regulated tyrosine kinase substrate. *Hum. Mol. Genet.*, **11**, 3167–3178.
51. Cheng, H.L., Steinway, M., Delaney, C.L., Franke, T.F. and Feldman, E.L. (2000) IGF-I promotes Schwann cell motility and survival via activation of Akt. *Mol. Cell. Endocrinol.*, **170**, 211–215.
52. Faruqi, T.R., Gomez, D., Bustelo, X.R., Bar-Sagi, D. and Reich, N.C. (2001) Rac1 mediates STAT3 activation by autocrine IL-6. *Proc. Nat. Acad. Sci. USA*, **98**, 9014–9019.
53. Simon, A.R., Vikis, H.G., Stewart, S., Fanburg, B.L., Cochran, B.H. and Guan, K.L. (2000) Regulation of STAT3 by direct binding to the Rac1 GTPase. *Science*, **290**, 144–147.
54. Bromberg, J.F., Wrzeszczynska, M.H., Devgan, G., Zhao, Y., Pestell, R.G., Albanese, C. and Darnell, J.E. Jr (1999) Stat3 as an oncogene. *Cell*, **98**, 295–303.
55. Gutmann, D.H., Giordano, M.J., Fishback, A.S. and Guha, A. (1997) Loss of merlin expression in sporadic meningiomas, ependymomas and schwannomas. *Neurology*, **49**, 267–270.
56. Dahlberg, W.K., Little, J.B., Fletcher, J.A., Suit, H.D. and Okunieff, P. (1993) Radiosensitivity in vitro of human soft tissue sarcoma cell lines and skin fibroblasts derived from the same patients. *Int. J. Radiat. Biol.*, **63**, 191–198.
57. Huynh, D.P. and Pulst, S.M. (1996) Neurofibromatosis 2 antisense oligodeoxynucleotides induce reversible inhibition of schwannomin synthesis and cell adhesion in STS26T and T98G cells. *Oncogene*, **13**, 73–84.